X-552-70-96
PREPRINT

GEODETIC EARTH ORBITING SATELLITE (GEOS-C)—APPLICATIONS TECHNOLOGY SATELLITE (ATS-F) TRACKING EXPERIMENT

THEODORE L. FELSENTREGER
THOMAS J. GRENCHIK
PAUL E. SCHMID

MARCH 1970

GSFC
GODDARD SPACE FLIGHT CENTER
GREENBELT, MARYLAND

GEODETIC EARTH ORBITING SATELLITE (GEOS-C) - APPLICATIONS TECHNOLOGY SATELLITE (ATS-F) TRACKING EXPERIMENT

Theodore L. Felsentreger
Thomas J. Grenchik
Paul E. Schmid

and

The Johns Hopkins University—Applied Physics Laboratory
Communications and Systems, Inc.

March 1970

MISSION & TRAJECTORY ANALYSIS DIVISION
GODDARD SPACE FLIGHT CENTER
Greenbelt, Maryland

CONTENTS

CONTENTS (cont'd.)

CONTENTS (cont'd.)

GEODETIC EARTH ORBITING SATELLITE (GEOS-C) - APPLICATIONS TECHNOLOGY SATELLITE (ATS-F) TRACKING EXPERIMENT

I. EXPERIMENT OBJECTIVES

The scientific and technical objectives of the GEOS-C/ATS-F tracking experiment are as follows:

1. The obtaining of more precise information about the value of satellite-to-satellite tracking for geodesy. The utility of continuous spans of tracking data covering half an orbit of GEOS-C will be studied. For example, evidence for gravity anaomalies will be sought. These results will be correlated with the experience provided by the NIMBUS-E/ATS-F experiment.

2. The precise evaluation of the orbit determination technique involving the tracking of a near-earth satellite from a synchronous satellite, and the precise evaluation of the performance of the satellite-to-satellite tracking system.

3. The conducting of intercomparison experiments involving the satellite-to-satellite tracking system and other tracking systems on GEOS-C and ATS-F.

4. The evaluation and use of the satellite-to-satellite tracking capability and the radar altimeter capability for the purpose of conducting earth physics studies, including oceanographic studies. This will include joint experimental activities and analyses involving the GEOS-C altimeter and satellite-to-satellite tracking between the ATS-F and GEOS-C spacecraft. Correlations between altimeter measures and satellite-to-satellite tracking data will be looked for.

The orbits of the GEOS-C spacecraft determined on the basis of its conventional tracking systems will be known with greater accuracy than those of any other near-earth satellite which could be used with ATS-F in a satellite-to-satellite tracking and orbit determination experiment. For example, it is anticipated that both the GEOS-C and the ATS-F spacecraft will be fitted with laser corner reflectors. This will make possible the determination of precise orbital positions for both spacecraft in an independent manner, and the conducting of precision orbital and tracking system

intercomparison studies involving the two satellites of a type which cannot be carried out if both spacecraft are not equipped with laser corner reflectors.

The practicability of improving the accuracy of range rate tracking data to, say, a tenth of a millimeter per second using measuring intervals ten to fifty seconds long will be investigated.

The operation of the GEOS-C does not involve control jet actions. Hence, reference standard orbits of any required length can be obtained without any of the complications associated with control jet operation. It is expected that reference standard orbits at least a week in length and perhaps as long as a month in length will be used in the analyses.

On the basis of these factors, then, as was pointed out in Reference 1, GEOS-C is the ideal satellite for providing the reference standard orbital information which will be essential for the proper evaluation of the satellite-to-satellite tracking and orbit determination techniques and their potential application to geodetic problems.

II. SIGNIFICANCE

A. Scientific and Technological

The more continous tracking coverage afforded by the GEOS-C/ATS-F link will prove advantageous insofar as geodetic investigations and orbit determination are concerned. In particular, solutions for the geopotential of the earth will be strengthened by the more extensive coverage than was obtained with previous geodetic satellites. Better knowledge of the earth's gravitational field will then aid in the orbit determination of GEOS-C, and, indeed, of all other artificial earth satellites.

Since satellite orbit determination is now based on the use of multiple short arc tracking data spans from many tracking stations, the longer data arcs obtained via the GEOS-C/ATS-F link should enhance the orbit determination of GEOS-C itself. In addition, the link is essentially another tracking system providing additional tracking data to be combined with data from conventional ground based systems. This should further strengthen the orbit determination of GEOS-C.

The enhanced tracking coverage obtainable by the GEOS-C/ATS-F link should also strengthen intercomparison studies of the various tracking systems involved in the whole project.

There will be common periods of time during which altimeter data and satellite-to-satellite tracking data will be obtained. This will allow correlative studies involving altimeter measurements and satellite-to-satellite tracking data to be made.

B. Operational

Present tracking of artificial earth satellites is normally accomplished only by networks of earth based systems. For fairly low satellites, such as GEOS-C will be, tracking coverage from a single station is limited to a few minutes per orbit. Therefore, to obtain relatively complete global tracking coverage for such satellites, extensive networks of tracking stations all around the earth have been established. Such networks are quite costly in terms of the instrumentation needed and the manpower involved in operating the networks. Also, because of the geographical locations of the stations, some networks are unable to provide adequate coverage of satellites having certain orbital characteristics.

A tracking system involving satellite-to-satellite tracking would help solve many of these problems. In many cases, such a system could perform many of the key functions of the ground based tracking stations, thus reducing instrumentation and manpower requirements. Also, each satellite in the tracking system would be able to track a particular spacecraft for a much longer period of time than an earth based station, thereby reducing the difficulties which may be involved in sequential tracking by multiple ground stations (Reference 2).

The tracking of GEOS-C from ATS-F will aid in determining the feasibility of establishing such a Tracking and Data Relay Satellite System (TDRSS). Since ATS-F will be in a synchronous orbit, it will be able to track GEOS-C over more than half of each GEOS-C orbit.

III. DISCIPLINARY RELATIONSHIPS

A. Related Scientific Work

1. NIMBUS-E/ATS-F Experiment

There will be a similar tracking and data relay experiment involving a link between NIMBUS-E and ATS-F (References 3 & 4). Each of the two experiments has its own particular advantages and disadvantages as discussed below.

a. Orbital Maneuvers

i. The NIMBUS-E orbit will be frequently perturbed by the firing of jets, thereby limiting the usefulness of some of the tracking data for geodetic purposes.

ii. The GEOS-C orbit will be free of jet firing. This means that essentially all of the tracking data are potentially useful for geodetic purposes.

b. Other Tracking Coverage

i. In addition to the link to ATS-F, the NIMBUS-E satellite will be tracked only by the STADAN ground sites.

ii. Tracking of GEOS-C, in addition to the ATS-F link, will be performed by optical, laser, Tranet, C-Band, USB, and STADAN systems. The orbit of GEOS-C will thus be known with geodetic accuracy on the basis of conventional ground tracking. This will permit evaluation of the GEOS-C/ATS-F tracking data from the standpoints of geodesy and precise orbit determination.

c. Orbital Characteristics

i. NIMBUS-E will be in a near-polar orbit. Thus, very nearly complete global coverage sensing of the earth's gravitational field will be obtainable via the NIMBUS-E/ATS-F link. In addition, the NIMBUS-E/ATS-F experiment would provide tracking data while NIMBUS-E is traveling nearly perpendicular to the earth's equator.

ii. GEOS-C will be in a rather low inclination orbit (about 20°). Tracking data will thus be obtainable while the satellite is traveling approximately parallel to the equator. This will permit an additional type of sensing of the earth's gravitational field.

d. Tracking Geometry

i. NIMBUS-E can be tracked continuously all around its orbit approximately twice a day by ATS-F. Also, ATS-F will be able to provide tracking data both in, and perpendicular to, the orbital plane of NIMBUS-E. This coverage will strength the orbit determination solutions.

ii. Perturbations in mean anomaly and altitude will be observable all around the orbit of GEOS-C in the course of a day.

e. Technology

i. NIMBUS-E will receive the signal from ATS-F by means of an antenna installed on a steerable mount so that the antenna can point toward ATS-F.

ii. GEOS-C will be equipped with a phased array which has the advantage of simplicity.

B. Present State of the Art

1. Current Programs

a. Geodetic tracking—optical and electronic means are presently being used to track artificial earth satellites for geodetic purposes. However, these means are all tied to earth-based tracking systems. Satellite-to-satellite tracking will add another dimension to geodetic tracking of earth satellites. In addition, tropospheric and some ionospheric refraction problems can be avoided on GEOS-C/ATS-F paths.

b. Selenodetic tracking—tracking data from the five Lunar Orbiters, the several Apollo spacecraft, and the Anchored IMP-E have all been used to improve our knowledge of the moon's gravitational field. The tracking coverage of a lunar orbiting spacecraft from an earth-based station is very similar to that which will be

realized by earth satellite-to-satellite tracking in that continuous data for about half an orbit will be received. The experience gained in analyzing such data for the lunar case will prove useful when GEOS-C/ATS-F and NIMBUS-E/ATS-F tracking data is available.

c. Lunar laser corner reflector—the placing of laser corner reflectors on the moon by the Apollo Project has provided scientists with a means for improving our knowledge of such things as the earth-moon distance, lunar librations, polar motions, and variations in the earth's rotational rate.

2. Future Geodetic and Selenodetic Efforts

a. VLBI (Very Long Baseline Interferometry)

b. Drag-free satellites

c. Satellite-to-satellite tracking between two satellites in nearly the same low altitude orbit, but separated by mean anomaly.

d. ATS-F/ATS-G tracking. This will be another step towards eventual establishment of a TDRSS.

e. Lunar satellite-to-satellite tracking with one spacecraft stationed at, say, the L2 libration point. This will provide previously unavailable lunar backside tracking data, which will greatly improve our knowledge of the moon's gravity field.

f. Laser tracking of future spacecraft.

IV. EXPERIMENTAL APPROACH

A. Experimental Concept

The ATS-F spacecraft will be in a geo-synchronous orbit, while GEOS-C will have a much lower orbit at a proposed inclination of about 20°. Consequently, ATS-F will be able to "see" GEOS-C for more than half of each GEOS-C orbit.

Basically, the link will operate in the following manner: the initial signal will be transmitted from an ATS-F ground station to the ATS-F spacecraft, where it will be converted to the proper mode for reception by GEOS-C. The converted signal will then be transmitted to GEOS-C, where it will be reconverted for transmission back to ATS-F and thence to the ATS-F ground station via the same instrumentation. The final data will take the form of range and range rate sums (Figure 4-1).

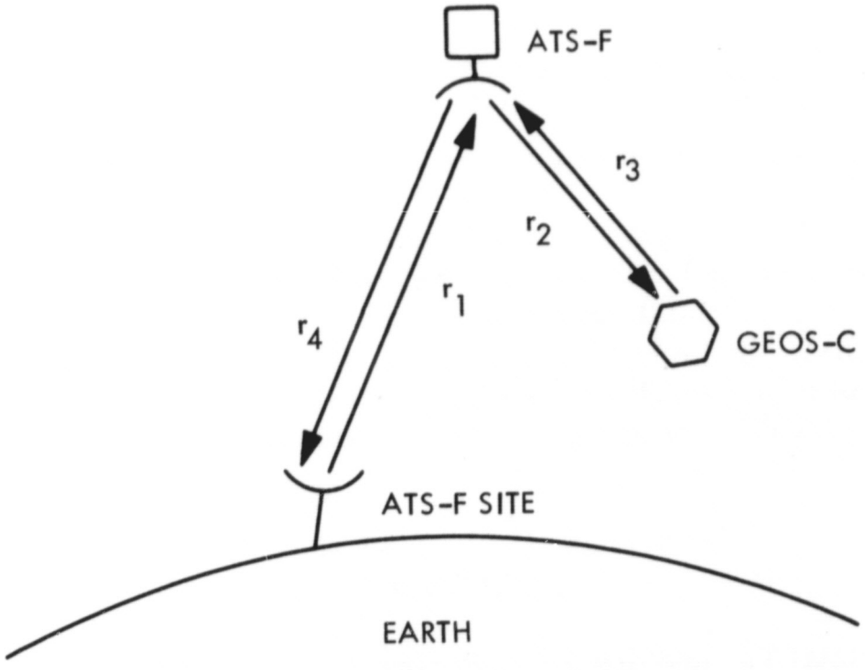

Figure 4-1. GEOS-C/ATS-F Link

Range sum = $r_1 + r_2 + r_3 + r_4$

Range rate sum = $\dot{r}_1 + \dot{r}_2 + \dot{r}_3 + \dot{r}_4$

Because of the short time intervals involved between transmission, reception, and retransmission of signals, it is convenient for many purposes to view the measurement process in terms of only two ranges and two range rates. Thus,

Range sum = $\rho_1 + \rho_2$

Range rate sum = $\dot{\rho}_1 + \dot{\rho}_2$,

where $\rho_1 = \frac{1}{2}(r_1 + r_4)$ and $\rho_2 = \frac{1}{2}(r_2 + r_3)$

B. Procedures and Methods

1. Orbital Considerations for GEOS-C/ATS-F

The proposed GEOS-C orbit will be 926 by 1204 km.with a 20-degree inclination, and ATS-F will be in a synchronous equatorial orbit. Orbital parameters for a nominal 926 by 1204 km. orbit are listed in Table 4-1. Figure 4-2 illustrates that the zone of visibility of possible ATS-F locations relative to GEOS-C is approximately ±122 degrees along the orbital plane and ±24.3 degrees across the

TABLE 4-1

Orbital Parameters for a Nominal 926 by 1204 km. Orbit

Perigee Radius	7301 km.
Apogee Radius	7579 km.
Semi-Major Axis	7440 km.
Eccentricity	.019
Perigee Velocity	7.4569 km./Second
Apogee Velocity	7.1838 km./Second
Period	106.5 Minutes

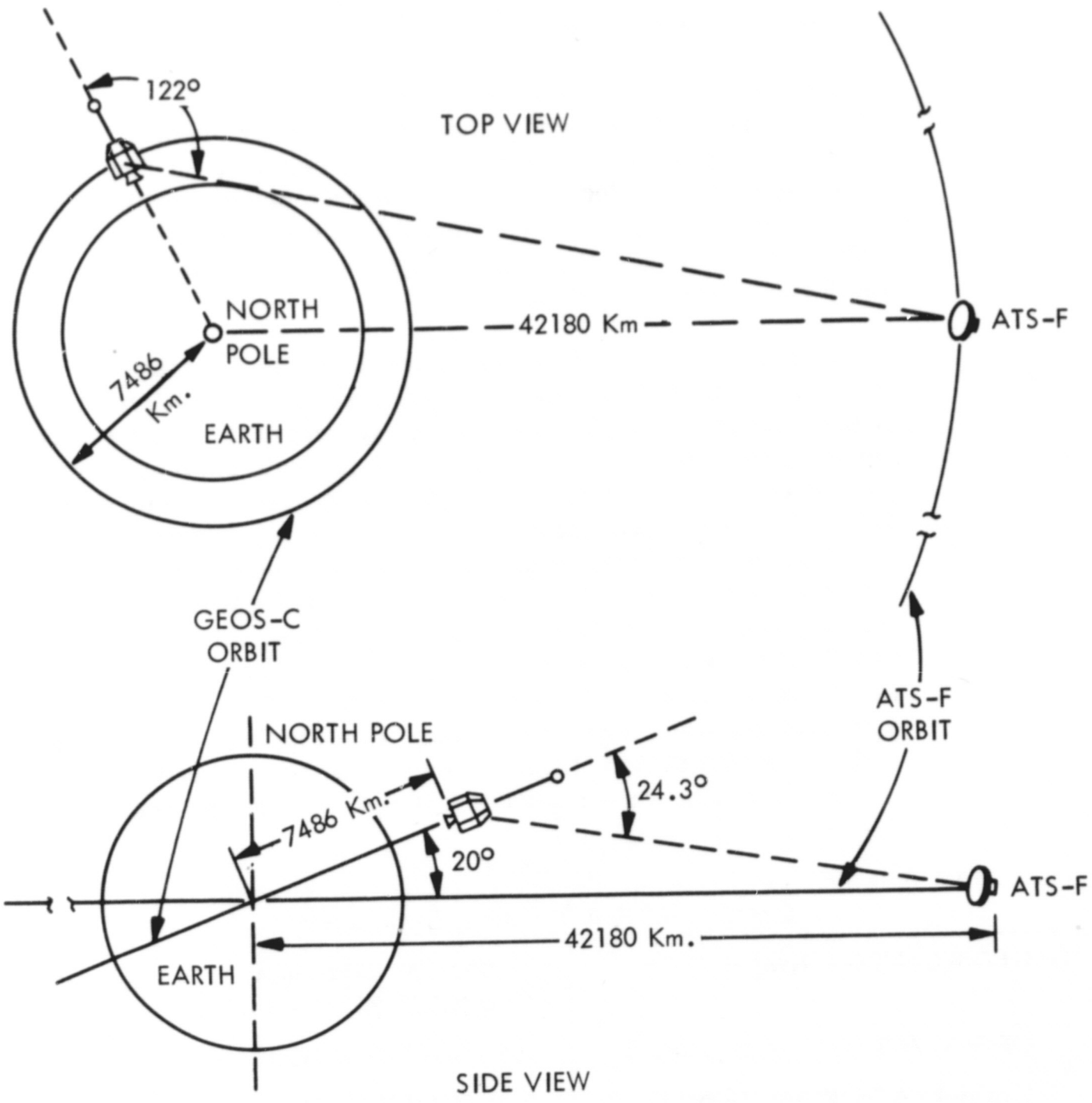

Figure 4-2. GEOS-C/ATS-F Orbital Geometry

orbital plane. However, tracking accuracy will be degraded by refraction of the RF energy as it passes through the earth's atmosphere when GEOS-C is near the horizon. Tracking over an arc which does not require the RF energy to pass through the atmosphere could limit tracking to approximately 60% of the orbital period, or for 1 hour.

The maximum angle across the orbit plane will be less than ±24.3 degrees for passes in which ATS-F is near the orbit plane of GEOS-C. This angle will be about ±3 degrees for a 20-degree inclined orbit, and ±4 degrees for a 30-degree inclined orbit. Therefore, the experiment can be performed during selected passes with orbit inclinations greater than 20 degrees and narrow antenna beamwidth across the orbit plane.

Maximum velocity and acceleration of GEOS-C relative to ATS-F must be considered in some cases for tracking GEOS-C via ATS-F. Doppler frequency shift of the RF energy received by GEOS-C corresponds to velocity, and Doppler frequency rate corresponds to acceleration. Maximum velocity of 7.4569 km./second occurs when GEOS-C is at perigee and its velocity vector is pointing toward ATS-F. Maximum acceleration of 7.96 m/second/second occurs as GEOS-C passes beneath ATS-F, or as its velocity relative to ATS-F goes through zero, and GEOS-C is at perigee. These values correspond to a Doppler frequency shift of 44kHz and a Doppler rate of 47 Hz/second respectively for a nominal 1800 MHz uplink carrier frequency. Maximum allowable one-way Doppler frequency shift for tracking with a standard GRARR transponder is ±85 kHz (reference 11). Table 4-2 tabulates the expected GEOS-C/ATS-F tracking parameters.

TABLE 4-2

GEOS-C/ATS-F Tracking Parameters

GEOS-C/ATS-F Range, R	35,000 KM (Minimum) 45,000 KM (Maximum)
GEOS-C/ATS-F Range Rate, $\dot{R}$	7.5 KM/SEC (Maximum)
GEOS-C/ATS-F Acceleration, $\ddot{R}$	0.01 KM/SEC^2 (Maximum)
ATS-F Pointing Angle	10 DEG (Maximum angle off boresight to center of Earth)
ATS-F Angle Rate	.01 DEG/SEC (Maximum)
GEOS-C Pointing Angle	122 DEG (Maximum Angle off boresight)
GEOS-C Angle Rate	.09 DEG/SEC (Maximum)

2. Tracking Schedules

Here, the assumption is made that the available GEOS-C power supply will limit the maximum use of the ATS-F link to about 2 hours per day, or approximately 2 half-orbit passes of GEOS-C. Actually, GEOS-C will make about 13-14 orbits each day.

A feasible approach to using the maximum coverage time for geodetic purposes only would be to track 2 half-orbit passes each day separated by n non-tracked orbits, with n taking on any of the values 0, 1, 2, _ _ _ _, N-1, where N is the approximate number of GEOS-C orbits per day. This would result in the following set of possible tracking schemes for each day.

Orbit No.	1	2	3	4	5	6	7	_ _ _ _ _ _ _	N	N+1
n = 0	-	-								
1	-		-							
2	-			-						
.										
.										
.										
.										
N-1	-								-	

(Here, each line — indicates approximately half-orbit coverage using the ATS-F link.)

With any of these schemes, of course, GEOS-C would be tracked with the conventional ground-based systems before, during, and after the ATS-F covered passes.

Another possible scheme would be to systematically observe GEOS-C via ATS-F in all regions in which GEOS-C is not observed by any other tracking system. Such coverage would aid the orbit determination of GEOS-C.

It is planned to use the Caribbean region as the prime test area for the radar altimeter experiment, mainly because the ground-based tracking coverage is optimal as GEOS-C passes over this region. It would therefore be an advantage to obtain GEOS-C/ATS-F tracking data at the same time that altimeter measurements are made in the Caribbean area. This additional coverage would help strengthen the altimeter evaluation.

It would also be desirable to obtain GEOS-C/ATS-F tracking data during periods when altimeter measurements are made over other water areas where the ground-based tracking coverage is not so extensive (e. g., two approximately 30-minute passes per week over the Atlantic Ocean). These passes should be concurrent with the passes of GEOS-C during which altimeter data are obtained over the Caribbean area.

The colocation of the portable ATS-F ground station and a portable laser station at the Tananarive STADAN site, when the ATS-F satellite has been moved to its African location, might provide useful results for checking the accuracy of the range sums obtained through the GEOS-C/ATS-F links. When GEOS-C passes over Tananarive, the geometry would look something like that shown in Figure 4-3.

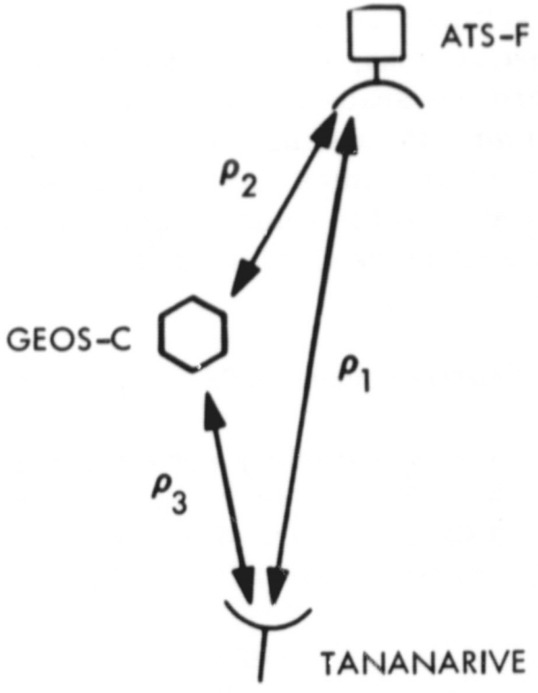

Figure 4-3. Tananarive Colocation Experiment Geometry

Then, $\rho_1 \simeq \rho_2 + \rho_3$, where the ρ_i's are ranges. Here, $\rho_1 + \rho_2$ would be measured by the GEOS-C/ATS-F system, ρ_1 would be measured by the ATS installation and the laser station, and ρ_3 would be measured by the STADAN site and the laser station.

C. Data Analysis

1. Evaluation of Tracking and Orbit Determination Systems

The orbits of both the GEOS-C and ATS-F spacecraft will be determined from conventional ground-based system data. In addition, the orbit of GEOS-C will be determined using the GEOS-C/ATS-F link tracking data. The differences between the two GEOS-C orbits will be examined and analyzed. There are other analyses which can be carried out, using different combinations of tracking data.

The major difficulty in precise orbit determination of the GEOS-C spacecraft via the tracking relay link lies in locating the synchronous spacecraft position with tolerable uncertainty. This type of error corresponds to the location uncertainty of a ground tracking station

and the resulting tracking error (Reference 7). For example, in the following paragraphs, a tabulation of the positional error of a present ATS synchronous spacecraft (spin stabilized) is given. Orbital errors in position for this existing synchronous spacecraft are listed below in terms of error studies such as in Reference 6, and also in terms of experience gained in actual orbit prediction with the orbit overlap techniques used in the GSFC Definitive Orbit Determination System (Reference 8).

Error Theory—Present ATS Position Errors

Using assumed tracking system errors of $\Delta R = \delta R = 15$m, and $\Delta \dot{R} = \delta \dot{R} = 0.5$ cm/s and simulated tracking of the ATS spacecraft of 24 hours (5 min. of 1 per sec. ($R + \dot{R}$)—tracking every 1/2 hour), one obtains total r.m.s. position errors of:

(1) $\Delta S = 300$ m
(2) $\Delta S = 1200$ m

ΔR and $\Delta \dot{R}$ are bias errors, and δR and $\delta \dot{R}$ are random. The value under (1) is based upon hypothetical tracking by Toowoomba and Mojave. That under (2) is based upon hypothetical tracking by Carnarvon and Toowoomba. The reason for the large difference in the error is the good tracking geometry of (1) (EW and NS separation), and the poor geometry of (2).

GSFC Experience—Present ATS Position Errors

Using real data, orbital overlap techniques, and the GSFC Definitive Orbit Determination System, the following r.m.s. position errors have been obtained in the past.

$$\Delta S = 1500 \text{ meters}$$

for a case in which Rosman and Mojave were used as tracking stations. This corresponds geometrically to the hypothetical Carnarvon-Toowoomba case described above under Error Theory.

As it can be seen, the theoretical and practical errors are in good agreement. The purpose here is to demonstrate that the theoretical error predictions are not too far off our practical values obtained recently. This gives some confidence in the error predictions shown below for the experiment proposed.

A similar study (simulated) was made for laser tracking of the proposed ATS-F spacecraft (cf. Reference 13). Positioning the spacecraft at 94° W longitude, the position error was 178 meters for the 2-station combination of Rosman and Mojave after a 24-hour period. When ATS-F is moved to 15° E longitude, it can be tracked by the portable laser station positioned at either Munich or Tananarive. After 24 hours of tracking, the position errors were 3300 meters and 2400 meters, respectively, for the two station locations.

Another analysis was performed to ascertain probable orbital errors for GEOS-C as tracked by the ATS-F link. Rosman was assumed to be the ATS ground station, the ATS-F spacecraft was placed at 94° W longitude, and a nominal 926 × 1204 km. orbit was assumed for GEOS-C. Range and range rate tracking was simulated for a 24-hr. period—the coverage by ATS-F was three 3-minute periods per GEOS-C pass, evenly distributed. The following additional assumptions were made:

Range noise = 8 meters

Range bias = 8 meters

Range rate noise = 1 cm./sec.

Range rate bias = 0.2 cm/sec.

Data sampling rate = 6/min.

(It should be noted that these error values reflect anticipated performance of the GEOS-C/ATS-F system.)

Figure 4-4 shows the position errors for ATS-F and GEOS-C, assuming no station location error for the ground station at Rosman. Figure 4-5 depicts the same thing, assuming a 60 meter location error for Rosman.

2. Intercomparison of Tracking Systems Using Satellite—Satellite Data

The more complete coverage afforded by the GEOS-C/ATS-F link will serve to strengthen and extend intercomparison results.

3. Geodetic Analysis

The GEOS-C/ATS-F link will provide much more complete tracking coverage over the global region between the latitudes plus and minus the inclination of the GEOS-C orbit. This data, combined with existing stores of geodetic data, should strengthen solutions for the gravity field of the earth.

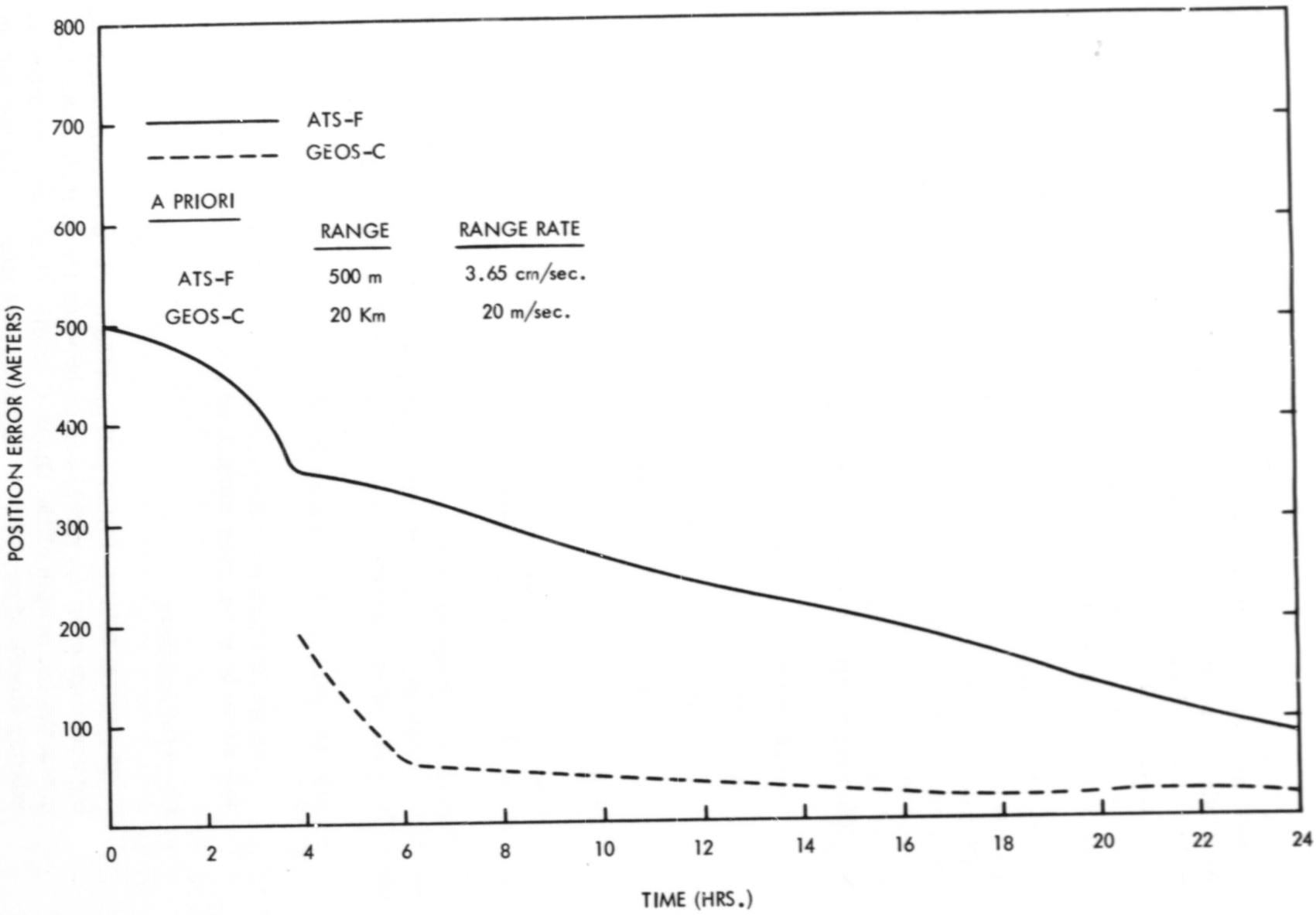

Figure 4-4. ATS-F and GEOS-C Position Errors (No Ground Station Location Error)

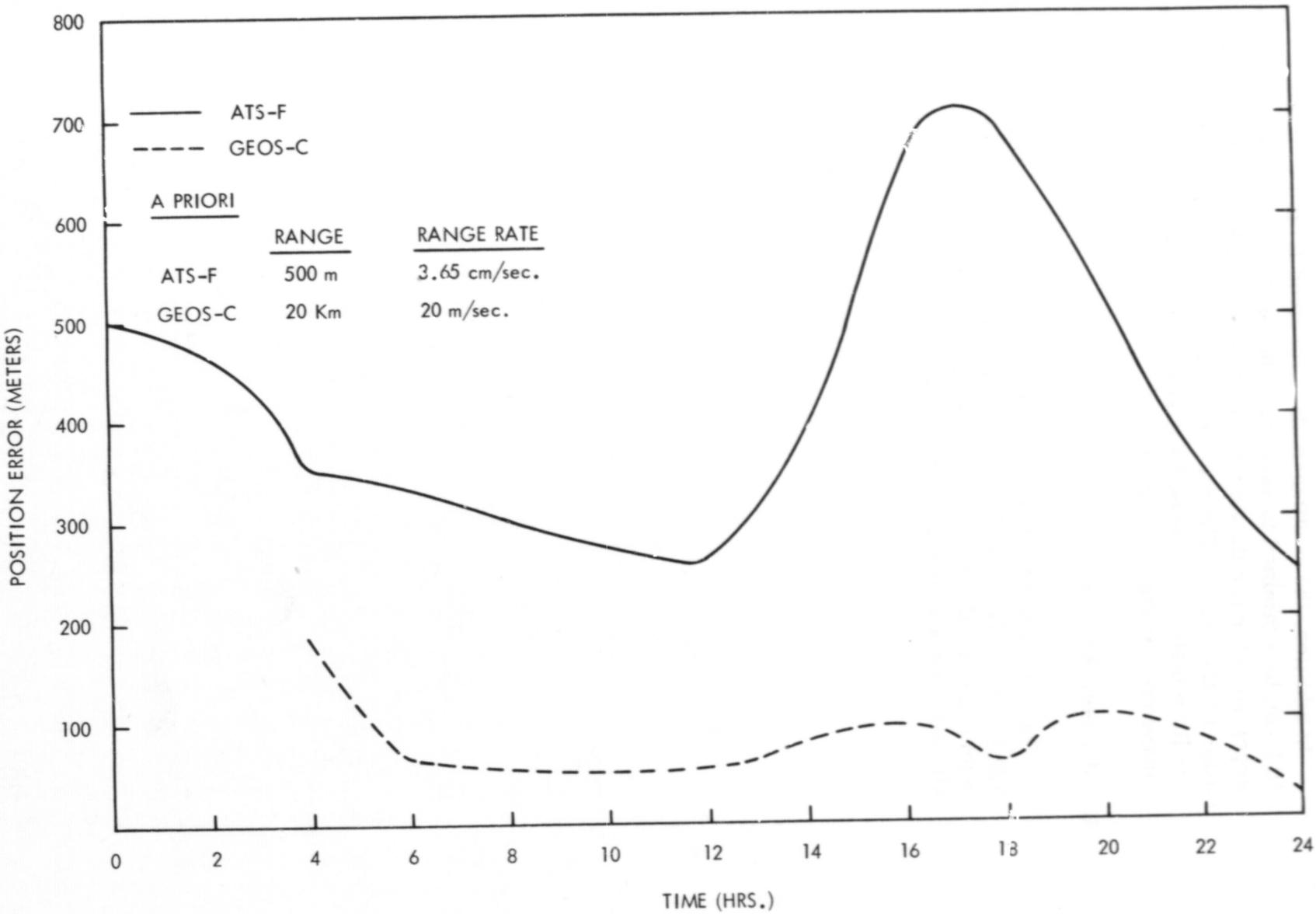

Figure 4-5. ATS-F and GEOS-C Position Errors (Ground Station Location Error =60 Meters)

In addition, the continuous data received from the GEOS-C/ATS-F link can be examined to ascertain the worth of GEOS-C as a direct accelerometer for the purpose of seeking evidence for gravity anomalies on the earth. The similar type of data obtained during the Apollo missions was used by various investigators to solve for lunar "mascons" (mass concentrations).

4. Altimeter Studies

The obtaining of altimeter data and simultaneous tracking coverage by the GEOS-C/ATS-F link while GEOS-C passes over the Caribbean area and the Atlantic Ocean will be carried out. The use of altimeter data in orbit determination will be investigated.

V. BASELINE OR CONTROL DATA

As was pointed out in Section IV, results obtained from the GEOS-C/ATS-F tracking data will be compared with results obtained from tracking of GEOS-C by conventional ground-based systems (i. e., optical, laser, Tranet, C-band, USB, and STADAN).

In addition, the GEOS-C/ATS-F link will be used as an aid in evaluating the radar altimeter by contributing tracking coverage simultaneously with altimeter measurements over water areas.

VI. ENGINEERING AND HARDWARE

A. Introduction

The proposed experiment will demonstrate the feasibility of tracking a spacecraft in a near earth orbit with geodetic precision via a synchronous satellite. In this experiment the near earth orbiting satellite will be GEOS-C and the synchronous satellite will be ATS-F. An experiment tracking NIMBUS-E via ATS-F is planned (Reference 3), and the proposed GEOS-C experiment will be compatible with the ATS-F hardware and link and will utilize the transponder technology developed for NIMBUS. Therefore, no modifications to the ATS-F spacecraft are contemplated. The position of GEOS-C will be precisely determined by other onboard instrumentation and its orbit will not be affected by mass expulsion forces, thus providing an excellent method for evaluating the technique of precisely tracking a low-orbiting satellite from synchronous altitude.

Three approaches were investigated for implementation of the tracking relay transponder on GEOS-C. These were:

Standard Goddard Range and Range Rate (GRARR) transponder augmented with a low noise RF input amplifier and a RF output power amplifier, and a relatively high gain (~6dB) antenna array. This approach was chosen for implementation.

GRARR transponder modified to include range tone filtering in one channel, a RF output power amplifier, and a lower gain antenna (~3dB). This approach was discarded because the large potential delay variation through the modified transponder range tone filter would jeopardize the range measurement.

Phase locked loop transponder (i.e., SGLS type) with a RF power amplifier and a low gain antenna (~0dB). This concept provides range rate tracking accuracies equivalent to the GRARR transponder but poorer range tracking accuracies with the 0dB antenna gain. This approach was not considered acceptable because of the additional difficulties in loop acquisition, with no significant improvement in range tracking over the GRARR transponder (if both approaches used a 6dB antenna gain).

B. Tracking Link Analysis and Investigation of the Augmented GRARR Transponder

Proposed equipment for ATS-F, the synchronous satellite, includes a scanned S-Band antenna system and a coherent transponder for the relay of GRARR type tracking signals to and from NIMBUS-E. Instrumentation which is being submitted for approval for GEOS-C, the near-earth satellite, as a result of studies includes a transponder which incorporates both GRARR and Unified S-Band (USB) capability. A GRARR transponder has been flown on the GEOS-A and GEOS-B spacecraft, and on GEOS-C will serve as the tracking relay transponder. The Unified S-Band (USB) transponder capability will permit ground tracking of GEOS-C from the Manned Space Flight Network (MSFN) stations. The experiment will make maximum use of existing space hardware and ground station facilities, will be compatible with ATS-F, and will cause a minimum impact on the design of GEOS-C.

In this section, the power budgets for the various links are also discussed, and the effects of augmenting the GRARR transponder and of several values of antenna gain are investigated. Possible methods for augmenting the transponder include use of a low noise pre-amplifier and addition of a RF output power amplifier. A low noise pre-amplifier is presently within the state of the art and is planned to be used on future GRARR transponders, and GSFC is investigating parametric amplifiers for use with the GRARR transponder. A 4 watt RF output power amplifier is planned for NIMBUS-E and a 10 watt amplifier is within the state of the art. Using nominal power budgets as bases, system performance in terms of range and range rate accuracy has been determined.

Power budgets for the links between the ATS-F and its ground site are the same as those given in Reference 3, and it is assumed that they are stronger than the satellite-satellite links. The utilization of GEOS-C in the system should have no effect upon the performance of the ground/ATS-F/ground links, consequently, these are not analyzed further. The GRARR GEOS-C/STADAN link has been previously demonstrated with the flights of both GEOS-A and -B. The links of interest in this analysis are those between ATS-F and GEOS-C.

The power budgets for the links between GEOS-C and ATS-F will not be the same as those given in Reference 3 for the NIMBUS-E/ATS-F. As indicated previously, it is planned to equip the NIMBUS spacecraft with a special quad helix articulated antenna which will be controlled

about two orthogonal axes by means of bi-axial gimbals. The gain of this antenna is to be in excess of 14 dB for received signals and 16 dB for transmitted signals. The basic power budgets for the ATS to GEOS and GEOS to ATS links, normalized for 0 dB antenna gain and 0 dBW ERP respectively, are shown in Table 6-1. They are the "nominal" power budgets but do include liberal allowances for "miscellaneous" loss, receiver loss, etc.

The analysis of the system with an augmented GRARR transponder reflects variations in input noise temperature, antenna gain, and transmitter RF output power. For this analysis, values assumed for these parameters are:

Noise temperature (T): 1200°, 600°, 300°

Antenna gain (G): 0, 3, 6, 9 dB

Output power (P): 1, 4, 10 watts.

Noise temperature of a transponder having a low noise preamplifier will be between the two upper noise temperatures assumed, and noise temperature using a parametric amplifier will be between the two lower values. Values chosen for output power are based on 1 watt for the standard transponder, 4 watts proposed for NIMBUS-E, and 10 watts as the maximum which could be reasonably supported by the GEOS electrical power system. Antenna gains were chosen to obtain a realistic spread of achievable values.

The GRARR transponder RF output carrier is generated in the transponder, and the modulation sidebands on the downlink signal are a function of the received uplink signal (see Appendix A). Curves relating output carrier and sideband power to S/N at the input to the limiter in the GRARR transponder have been developed (Reference 12). These curves, which are used to determine the share of the total RF output power in the phase modulation sideband, are shown in Figure 6-1. It can be noted that carrier power remains relatively constant while sideband power decreases rapidly as input S/N decreases below +10 dB. Validity of the curves has been verified by bench tests on a GRARR transponder (see Appendix E).

Table 6-1

Power Budgets
GEOS-C/ATS-F GRARR Power Budgets (Normalized)

ATS to GEOS	
Transmit Power	13.0 dBW
Antenna Gain	39.0 dB
Scanning Loss	-2.5 dB
Pointing Loss	-1.5 dB
Miscellaneous Loss	-0.5 dB
Scanning Network	-2.0 dB
Polarization Loss	-0.5 dB
Free Space Loss	-191.0 dB
Receiver Loss	-2.0 dB
Received Signal on a 0 dB antenna	-148.0 dBW
GEOS to ATS	
Free Space Loss	-192.5 dB
ATS Antenna Gain	+41.0 dB
Scanning Loss	-2.5 dB
Pointing Loss	-1.5 dB
Polarization Loss	-0.5 dB
Scanning Network and Line Loss	-3.5 dB
Miscellaneous	-2.5 dB
Received Signal for 0 dBW ERP at GEOS	-162.0 dBW
Receiver Noise in 550 KHz Noise Bandwidth:	-200.9 + 57.4 = -143.5 dBW

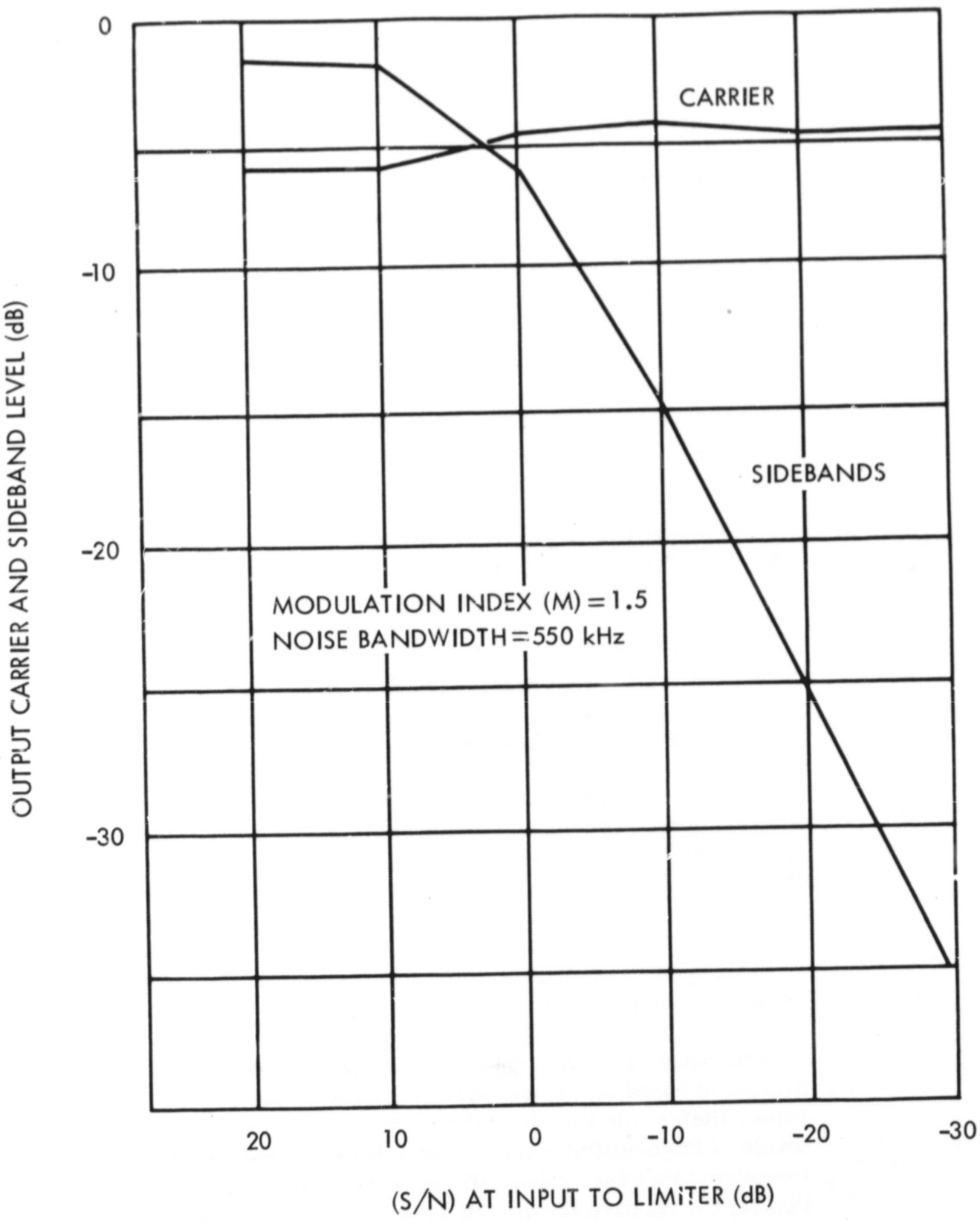

Figure 6-1. GRARR Transponder Output Carrier and Sideband Levels

The above parameters were exercised along with the normalized power budgets and the "suppression" of Figure 6-1 to derive a value for the sideband S/kT at the input to the ATS receiver for each case. An example of such a calculation is shown in Table 6-2.

The GRARR downlink sidebands are composed of the subcarrier which is derived from the uplink carrier, and the range tones which were modulated on the uplink carrier. Range accuracy is related to the power of the detected ranging tones only, therefore the power in the tones relative to total sideband power must be calculated. For one channel operation with a single tone, the level of each spectral line is 6.7 dB down from the unmodulated subcarrier level (reference 10), and total tone sideband power is 3.7 dB down relative to total sideband power. For one channel operation with dual tones, total power of the highest tone is 4.8 dB down relative to total sideband power.

The signal relayed back to the ground via ATS suffers some further degradation. For example, a limiter loss of approximately 1 dB occurs. Additional losses and noise, even though the ATS to ground link is very strong, may add another dB of S/kT degradation. Consequently, the range tone at the ground receiver is estimated to be 5.7 dB down from the sideband S/kT in the ATS receiver for single tone modulation, and highest tone level is estimated to be 6.8 dB down for dual tone modulation.

A graph of range instrumental accuracy versus range tone signal-to-noise power density in the ground receiver for a 1 Hz tracking bandwidth is shown in Figure 6-2 (Reference 10). This graph includes the error due to system resolution and the error due to thermal noise. The resolution error is constant for any one particular tone, and is about 2 meters for the 100 kHz tone. It can be noted from Figure 6-2 that system resolution is the limiting factor at signal-to-noise power densities greater than 45 dB.

The range rate error analysis for the satellite-satellite tracking system is based on the analysis presented in the General Dynamics report (Reference 10). In that report it was assumed that the relative levels of the downlink carrier and subcarrier remained constant. However, this assumption will not be valid at low input signal levels, that is, the relative levels will vary as shown in Figure 6-1 (Reference 12).

Table 6-2

Sample Calculation of GRARR Information
Sideband S/kt in ATS Receiver

GEOS Transponder Parameters: Noise Temp. 600°

Antenna 6 dB

Power 4 watts

In GEOS Transponder:

Received Carrier = -148 (from Table 6-1) + 6 (Antenna Gain)

= -142 dBW

Noise = -200.9 (Corresponds to 600°) + 57.4 (for 550 kHz noise bandwidth)

= -143.5 dBW

$(S/N)_{in}$ = -142 - (-143.5) = + 1.5dB

Therefore,

Sideband Signal Power = 5.5 dB down (from Figure 6-1)

Sideband Noise Power = 5.5 + $(S/N)_{in}$ = 7.0 dB down

In ATS Receiver:

Received Signal = -162 (From Table 6-1) - 5.5 (above) + 12 (ERP of GEOS)

= -155.5 dBW

Received Noise (radiated by GEOS) = -162 - 7.0 + 12 = -157.0 dBW

Thermal Noise in ATS = -143.5 dBW (Table 6-1)

Total Noise (Combined Thermal and Received) = -143.3 dBW

S/N = -155.5 - (-143.3) = -12.2 dB

S/kT = -12.2 + 57.4 (550 kHz noise bandwidth) = 45.2 dB - Hz

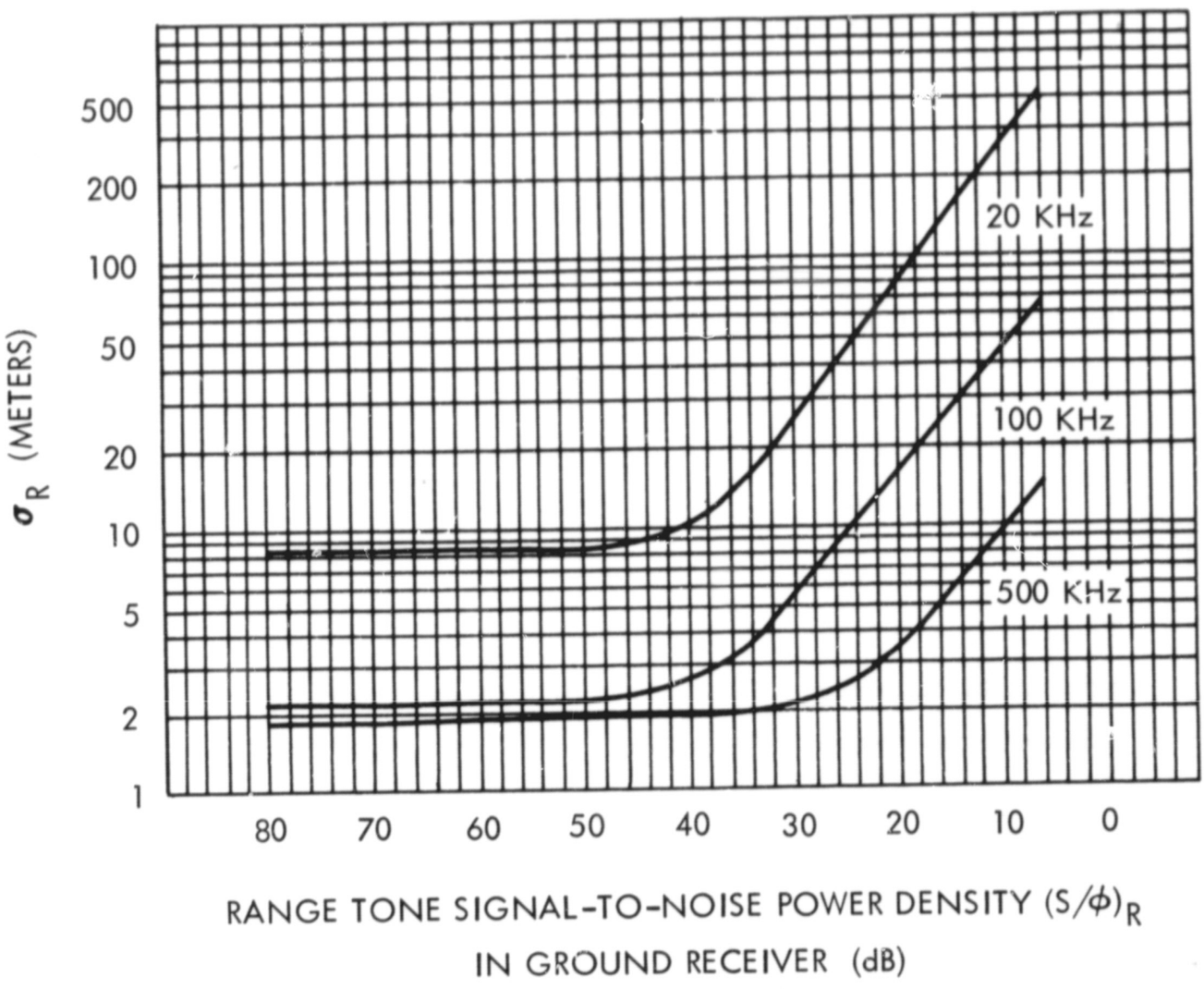

Figure 6-2. GRARR Range Instrumental Accuracy for 1 Hz Tracking Bandwidth (Reference 10)

The random error in range rate due to thermal noise is

$$\sigma_{\dot{R}_n} = \left[\frac{\lambda_t}{2}\right]\left[\frac{f_b + f_d}{2\pi N}\right]\left[\left(\frac{B_n \Phi}{S}\right)_C + \left(\frac{B_n \Phi}{S}\right)_{SC}\right]^{1/2}$$

where signal-to-noise power density (S/Φ) for the carrier and sub-carrier are calculated as described for the range error analysis. The total error ($\sigma_{\dot{R}}$) is the root sum square (RSS) combination of $\sigma_{\dot{R}_n}$ with the range rate resolution ($\sigma_{\dot{R}_r}$).

Values of various terms are:

$\frac{\lambda_t}{2}$ = 0.0833 meters (1800 MHZ) = half wavelength at ATS-F to GEOS-C frequency.

B_n = 10 Hz or 1kHz

sampling rate (sec^{-1})	$\frac{f_b + f_d}{2\pi N}$	$\sigma_{\dot{R}_r}$ (meters/sec)
4	1.700	0.034
2	0.850	0.017
1	0.486	0.00975
0.1	0.0356	0.00071

Range and range rate errors are listed in Appendix B for the various combinations of GRARR parameters and the following ground tracking station operating mode:

Single channel tracking
Range error (σ_R)

Range tone = 100 kHz
Tracking bandwidth = 1 Hz

Range rate error ($\sigma_{\dot{R}}$)

No range tone

Tracking bandwidth = 2 kHz (B_N = 1 kHz)

Sampling rate = 1/second.

Values of σ_R for several values of GRARR transponder input noise temperature (T) and RF output power (P) are (at a sample rate of 1/sec):

T (°K)	G (dB)	P (W)	σ_R (meters)	$\sigma_{\dot{R}}$ (meters/second)
1200	6	4	3.1	0.017
		10	2.7	0.014
600	6	4	2.7	0.016
		10	2.5	0.012

It should be noted that σ_R was calculated assuming that only the 100 kHz range tone is modulated on the uplink carrier and $\sigma_{\dot{R}}$ was calculated assuming that no range tones are modulated on the carrier. These conditions result in smaller errors than for other modulation conditions. In almost all cases, the error is less than twice the system resolution error.

The level of the signal received from ATS-F will generally not be sufficient to activate the transmitter in the GRARR transponder via the existing squelch gate. Therefore, a command capability will be required to activate the transmitter, and this may either replace or be connected in parallel with the squelch circuit.

C. GEOS Spacecraft Description

To date, two gravity gradient stabilized GEOS satellites have been launched, GEOS-I on 6 November 1965, and GEOS-II on 11 January 1968. Both spacecraft carried similar geodetic instrumentation, i.e., optical beacons, Sequential Collation of Range (SECOR) transponder, Goddard Range and Range Rate (GRARR) transponder, laser reflectors, and doppler beacons. In addition, GEOS-II carried two C-Band transponders, a passive radar reflector, and a CW laser detector.

A third GEOS satellite (GEOS-C) is being proposed for launch early in calendar year 1972. A 926 by 1204 Km. orbit with a 20 degree inclination is contemplated. Many of the proposed objectives of GEOS-C are similar to those of the predecessor GEOS satellites, with data planned for application to the NGSP objectives utilizing many of the same instrumentation systems. In addition, two new systems have been proposed for GEOS-C: a Unified S-Band (USB) transponder and a radar altimeter experiment.

The basic structure proposed for GEOS-C will be identical to its predecessors and will use the GEOS-II backup spacecraft. A side view of GEOS-II is shown in Figure 6-3. The top of the spacecraft is an 18 inch diameter attach ring which mates with the vehicle attachment fitting for launch; that is, the spacecraft is launched "up-side down." The gravity gradient damper and end mass are inside the spacecraft during launch, and the motorized boom is extended after orbit is achieved. Clearance for the damper and end mass is a 6 inch diameter area concentric with the attach ring. Battery power dump resistors and several small experiments were located between the damper clearance area and the attach ring on GEOS-I and -II. The major change which is presently proposed will be the installation of a parabolic reflector for the GEOS-C radar altimeter in place of the hemispherical broadband spiral antenna. The structure will limit the weight of GEOS-C to 500 pounds. An estimated weight breakdown of GEOS-C less the tracking relay experiment system for the GEOS-C/ATS-F experiment is presented in Table 6-3. Total estimated weight for the equipment listed is 426 pounds which allows 74 pounds for other instrumentation. Table 6-4 lists estimates of weight and volume for the tracking relay experiment system and Table 6-5 lists the power requirements (Reference 4).

The power system proposed for GEOS-C will be identical to the one in GEOS-I and -II which contained three separate subsystems, main, optical, and transponder. The GRARR transponder will be connected to the transponder subsystem which will include a 14.7 volt, 12 ampere-hour nickel-cadmium battery and a solar array capable of supplying approximately one ampere in sunlight. Depth of discharge of the battery for 1 hour of tracking in solar eclipse versus transponder power input is shown in Figure 6-4. Values for depth of discharge are slightly pessimistic because the solar eclipse period will be approximately 40 minutes. Maximum tracking duration for the proposed GEOS-C orbit will be approximately 1 hour. The C-Band transponders flown on GEOS-II have an input power of 25 watts or less during interrogation. If the GRARR transponder has an input power of 50 watts (4 watt RF nominal

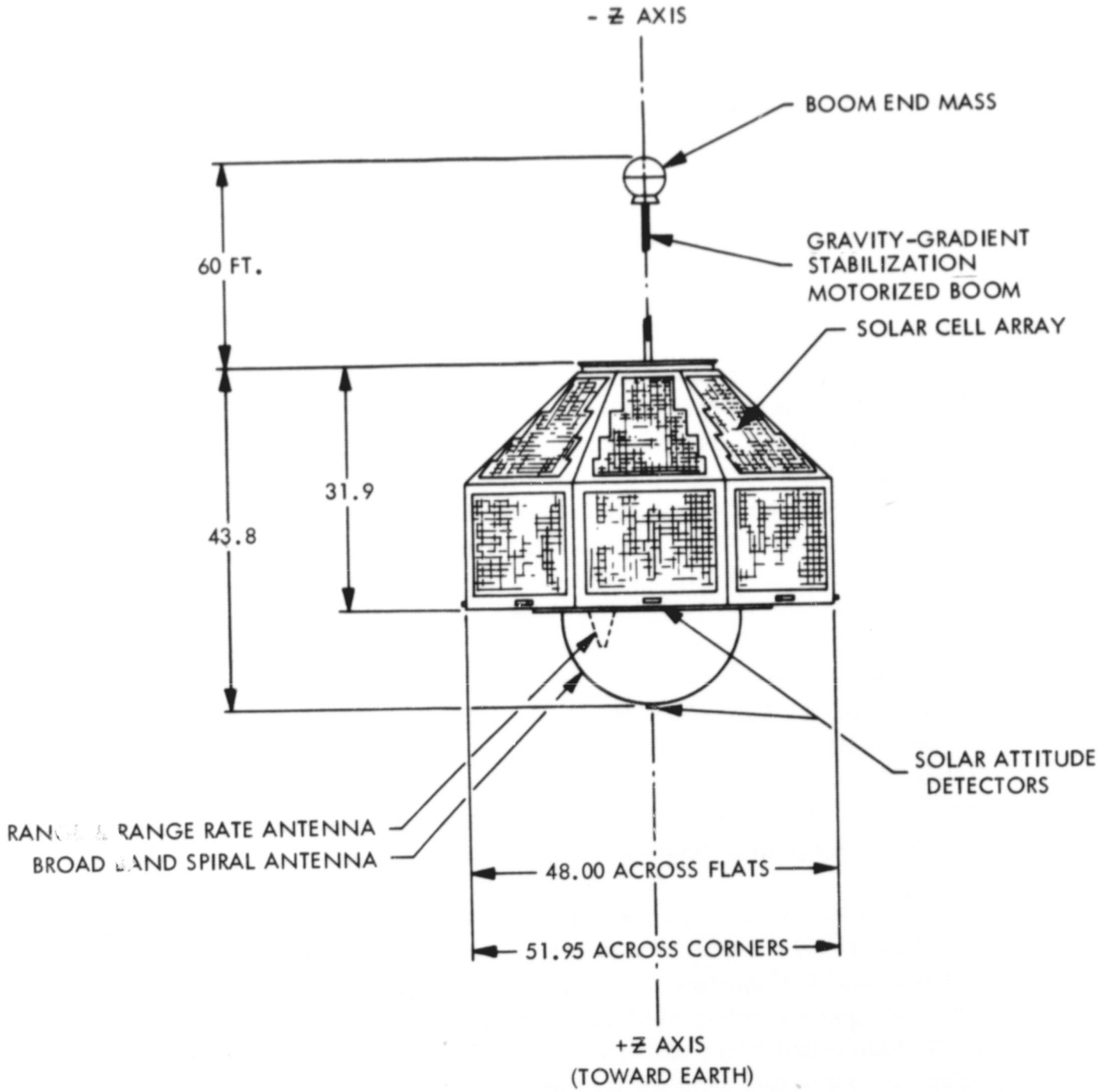

Figure 6-3. GEOS-II Side View Configuration

Table 6-3

GEOS-C Estimated Weight Breakdown Less GRARR

Item	Weight (pounds)
Structure	80
Power Supply	
Solar Array	20
Batteries (3)	55
Cabling	35
Instrumentation	
Doppler	11
Radar Altimeter	20
C-Band	8
USB	9
Optical Beacon	20
Laser Retroreflectors	11
Laser Detector	6
Van Atta Array	7
Antennas	12
Electronics	
Command	15
Telemetry	11
Memory	13
Thermal Control	30
Attitude Control (including yaw control)	38
Miscellaneous	25
TOTAL	426

Table 6-4

Estimated Weight and Volume for Tracking Relay Experiment System

	Weight	Volume
Basic Transponder (6 × 4 × 6.5 inches)	5.5 lbs.	156 $in.^3$
Power Amplifier (6 × 6 × 6.5 inches)	3.4 lbs.	234 $in.^3$
Digital Electronics (6 × 6 × 6.5 inches)	7.3 lbs.	234 $in.^3$

operation), and both the C-Band and GRARR transponders are continuously interrogated for the 1 hour pass duration, the depth of discharge of the battery will be approximately 31 percent. If the battery is fully charged at the start of the 1 hour tracking pass, this depth of discharge should not degrade battery reliability.

A momentum wheel has been proposed for GEOS-C. This wheel will tend to align the GEOS-C spacecraft so that the spin axis of the wheel is normal to the orbital plane. The wheel will provide gyroscopic stiffening about the roll axis and would provide the satellite with yaw control. It is estimated that yaw rotation can be held to ±10°. With GEOS-C in a low inclination orbit and yaw controlled, the required antenna array beam shape will be in the form of a fan approximately 50 degrees wide and ±122 degrees from the spacecraft vertical axis in the orbital plane. However, at angles greater than approximately ±100 degrees, the RF energy must pass through the earth's atmosphere.

If the spacecraft is launched into a higher inclination orbit, for example i = 30°, the antenna beam shape will have to be approximately 75° wide for complete coverage. However, by selecting a pass in which GEOS-C passes near the vertical through ATS-F, this restriction can be substantially reduced. For example, the maximum angle between the line from GEOS-C to ATS-F and the GEOS-C orbit plane for a pass in which GEOS-C passes beneath ATS-F is approximately 3° for i = 20°, and 4° for i = 30°.

Table 6-5

Estimated Power Requirements for Tracking
Relay Experiment System

MODULE	OPERATING MODE			
Basic Transponder Dissipation	Receive	Transmit Normal 4 Watts	Transmit Low 2 Watts	Transmit High 8 Watts
Receiver	1.5	1.5	1.5	1.5
Transmitter	0	1.0	1.0	1.0
Receiver DC Converter (75% efficiency)	.5	.8	.8	.8
Transmitter DC Converter (75% efficiency)	0	5.4	2.7	10.0
Sub Total	2.0	8.7	6.0	13.3
Digital Dissipation				
Command Detector/ Decoder*	1.15	1.15	1.15	1.15
Antenna Control	.75	.75	.75	.75
Link Evaluation	0	.20	.20	.20
Digital DC Converter (50% efficiency)	1.9	2.1	2.1	2.1
Sub Total	3.8	4.2	4.2	4.2
Power Amplifier†				
Dissipation	0	12.0	6.0	24.0
Total Dissipation	5.8	24.9	16.2	41.5
Total Power Input (Sum of dissipation & Transmitter Output)	5.8	28.9	18.2	49.5

*No dissipation if inhibited by command, also saves 1.15 watts of digital DC converter dissipation.

†25 percent DC to RF efficiency is assumed. This is a conservative estimate.

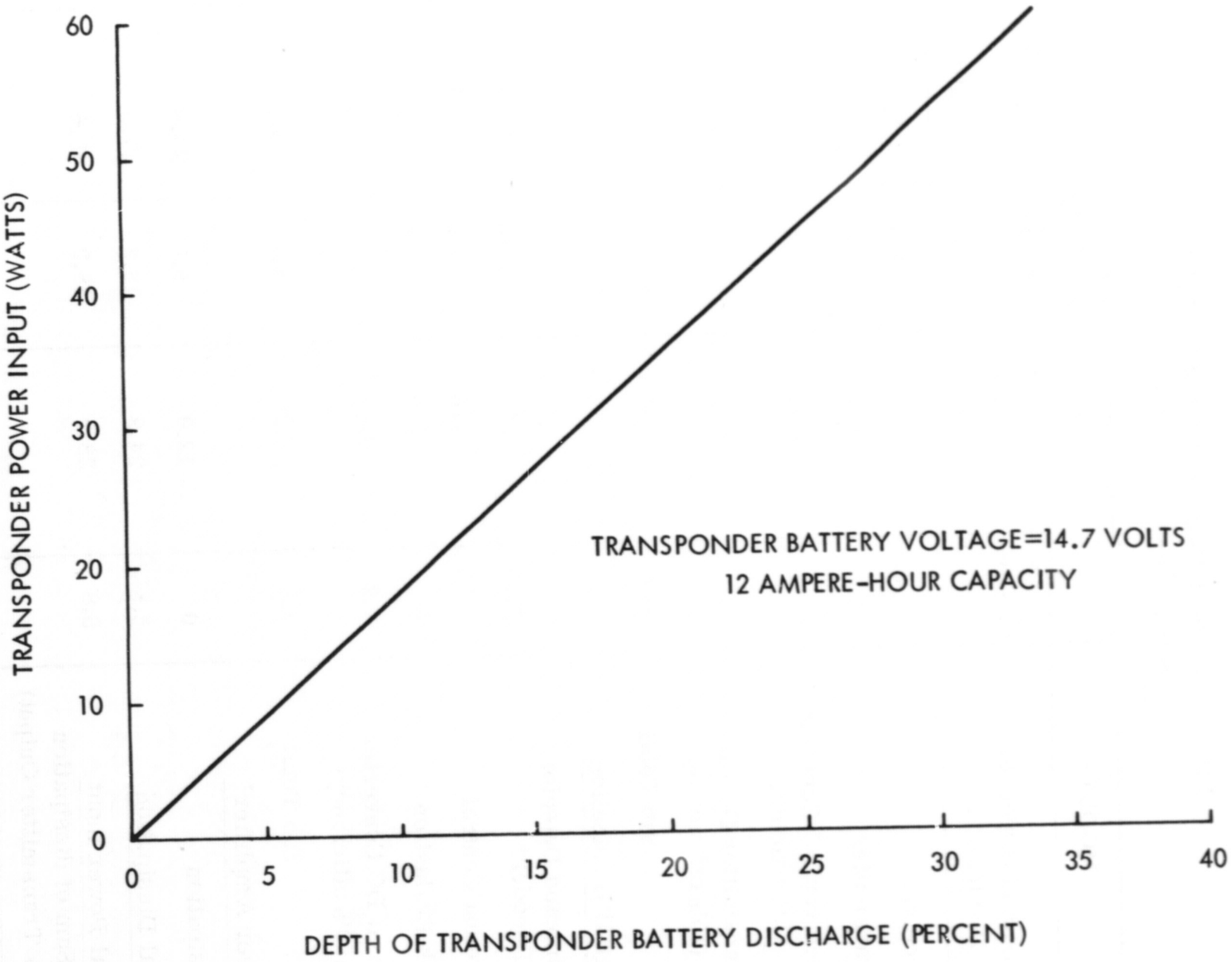

Figure 6-4. Depth of Transponder Battery Discharge For 1 Hour of Tracking in Solar Eclipse

The type of antenna proposed for NIMBUS-E would not be feasible with the GEOS-C spacecraft without extensive modification. It could not be mounted atop the spacecraft such as planned for NIMBUS, because it would interfere with the gravity-gradient rod and shadow portions of the solar arrays. In addition, the torques necessary to slew the antenna for tracking ATS-F would increase the libration amplitudes and may even cause the satellite to tumble. Several antenna concepts which are feasible for GEOS-C are discussed later.

D. Antenna Implementation

Installation on GEOS-C of a mechanically steerable antenna of the type which has been proposed for NIMBUS-E will not be feasible because it will interfere with the gravity gradient boom or shadow solar cells, and the torques induced will upset spacecraft stabilization. Antenna implementation on GEOS-C appears to be the major problem area for satisfactory performance of the tracking experiment, therefore, several possible approaches are considered. These approaches are the results of independent investigations carried out by the Johns Hopkins University/ Applied Physics Laboratory (APL) and by the Antenna Systems Branch of Goddard Space Flight Center. It has been assumed that GEOS-C will have yaw stabilization.

The top of the GEOS spacecraft when it is in orbit is the end which is attached to the vehicle during launch. The antenna concept suggested by APL would involve mounting five separate antennas on a modified hemisphere above the present attach ring (see Figure 6-5). In the launch configuration, an additional adapter section would fit over the array. Separation from the vehicle (Figure 6-5 (A-A)) would be accomplished first, then the additional adapter section would be jettisoned (B-B).

An antenna array of five independent elements selectable by a single-pole, five-position switch would satisfy the requirement of 6 dB antenna gain over 244° in the orbital plane and 48° across the orbit plane. The beamwidth of each element is a 60° cone. The elements are arranged in the in-orbit plane and the beams are shown in Figure 6-6. The beams of the elements cross-over at their 1.5 dB down points (at 40° intervals). The array, therefore, provides 6 dB gain over a beam measuring 60° in the cross-orbit plane (the element beamwidth) × 220° in the plane of the orbit (by selecting the element pointing at ATS/F). Because of the considerable overlap of the element beams, the exact time of switching from one to another will not be critical. Timing sequence can be initiated

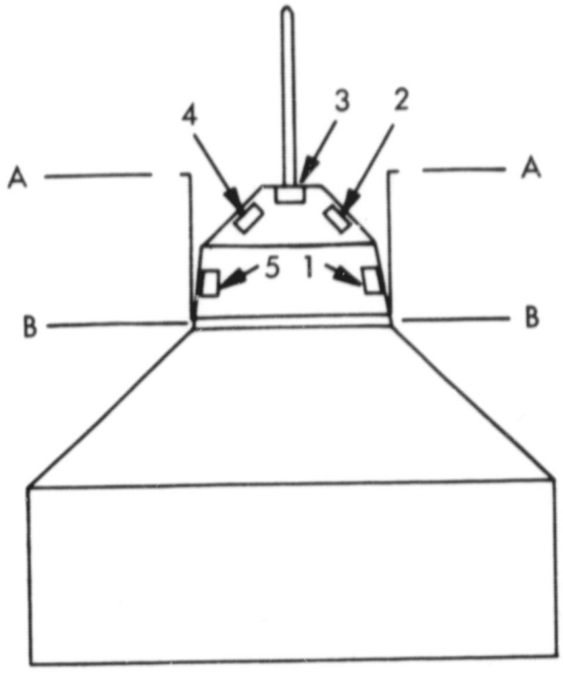

NOTE: ELEMENT 3 CAN BE HINGED TO PASS END MASS (LIKE DODGE) WITH CENTERED HOLD FOR BOOM OR CAN BE OFFSET TO SIMPLIFY MECHANICAL DESIGN.

Figure 6-5. Five Element Array on GEOS-C

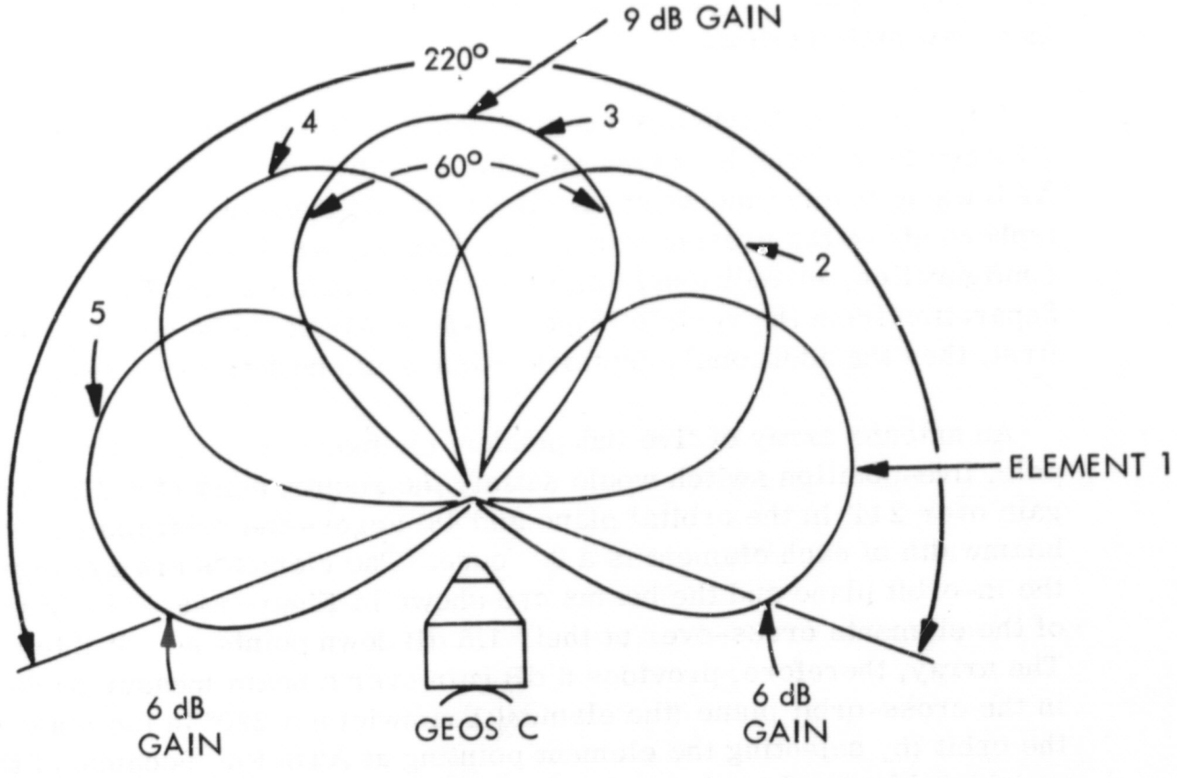

Figure 6-6. Element Patterns for Five Element Array

by real-time ground command or by a delayed command with variable delay time.

The antenna element which will provide the characteristics outlined above is the flat plate antenna. Such an element covering the 1.8 to 2.3 GHz frequency band would be a plate 4.0" on a side with a plate to ground-plane spacing of 0.25". The ground plane would be 8.0" square.

A major portion of the GEOS-C relay antenna design effort will be to integrate this antenna with the mechanical design of the spacecraft and the other antenna systems already on board. The design described in Figure 6-5 is structurally feasible. The array and switching network would be permanently mounted on the top side of the spacecraft with the array element pointing along the Z axis, offset to provide clearance for the boom and end-mass.

An antenna system suggested by GSFC would involve mounting an antenna array on each of the GEOS-C slant panels which are normal to the orbit plane (see Figure 6-7). Each array will generate four separate steerable beams resulting in the antenna patterns shown in Figure 6-8. It must be noted that the solar arrays on the slant panels would have to be redesigned, and solar power will be reduced slightly because the number of solar cells will be reduced. Each of the two antenna arrays consists of four cavity-backed spirals mounted on the GEOS slanting face. Each array is connected to a four-port Butler matrix which provides four overlapping beam positions along the array axis. The Butler matrix is connected to a single-pole four-throw diode switch which selects the desired antenna beam position upon command. A single-pole double-throw diode switch selects between the two beam-forming matrices, on either face of GEOS. The system block diagram for the antennas, Butler matrices, and switching networks is shown in Figure 6-9. Each block of the diagram is described in Appendix C.

After accounting for switch and matrix losses, array gain over 180° in the orbit plane and 50° across the orbit plane is approximately 3 dB or greater. Total antenna system weight less array supports is estimated to be 3.65 pounds and DC power requirement is estimated to 0.2 watts. An improvement to this approach might be to install two arrays side by side on each of the appropriate slant panels in order to increase the gain throughout the sector under consideration.

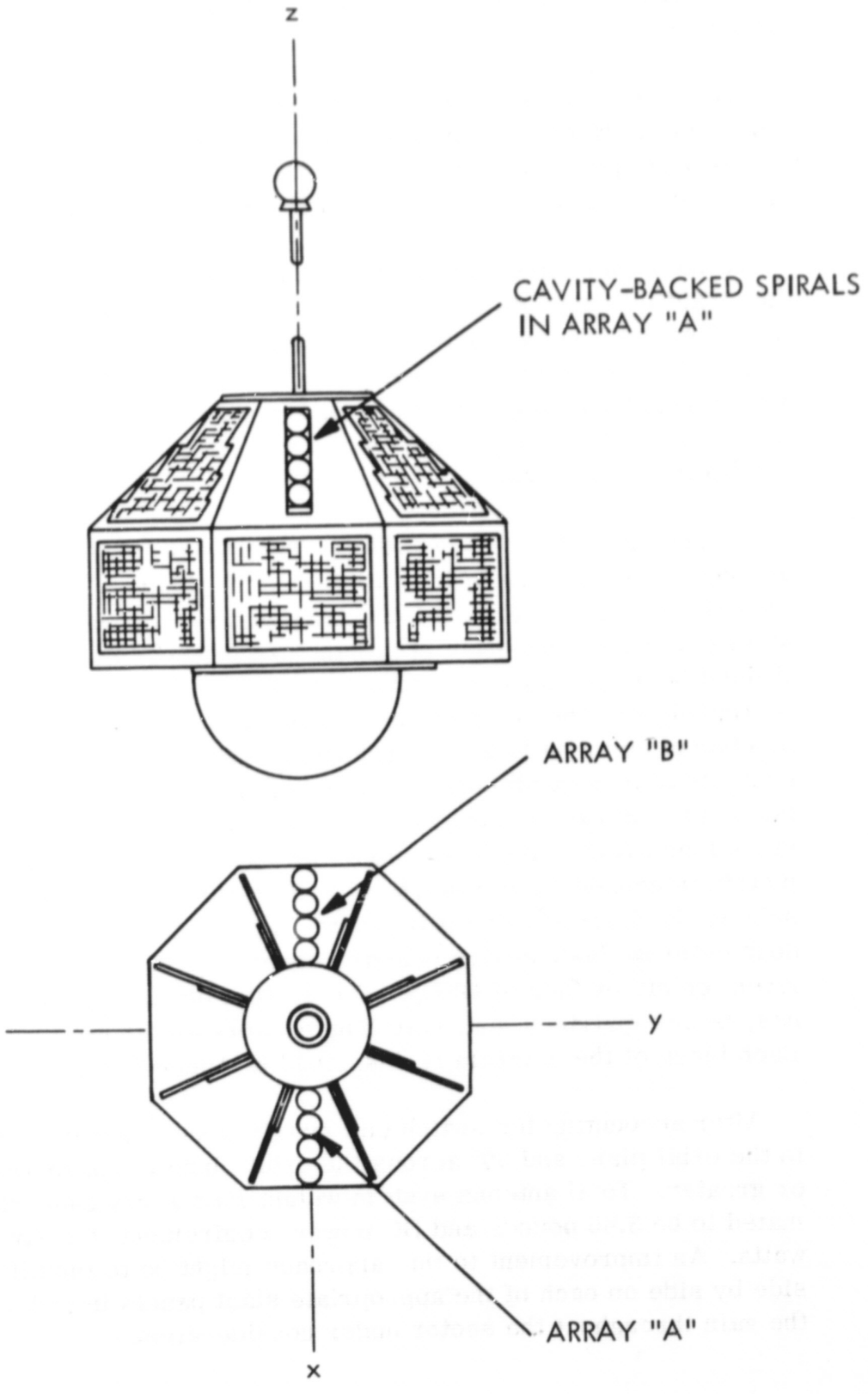

Figure 6-7. Two Electronically Steerable Arrays on GEOS-C

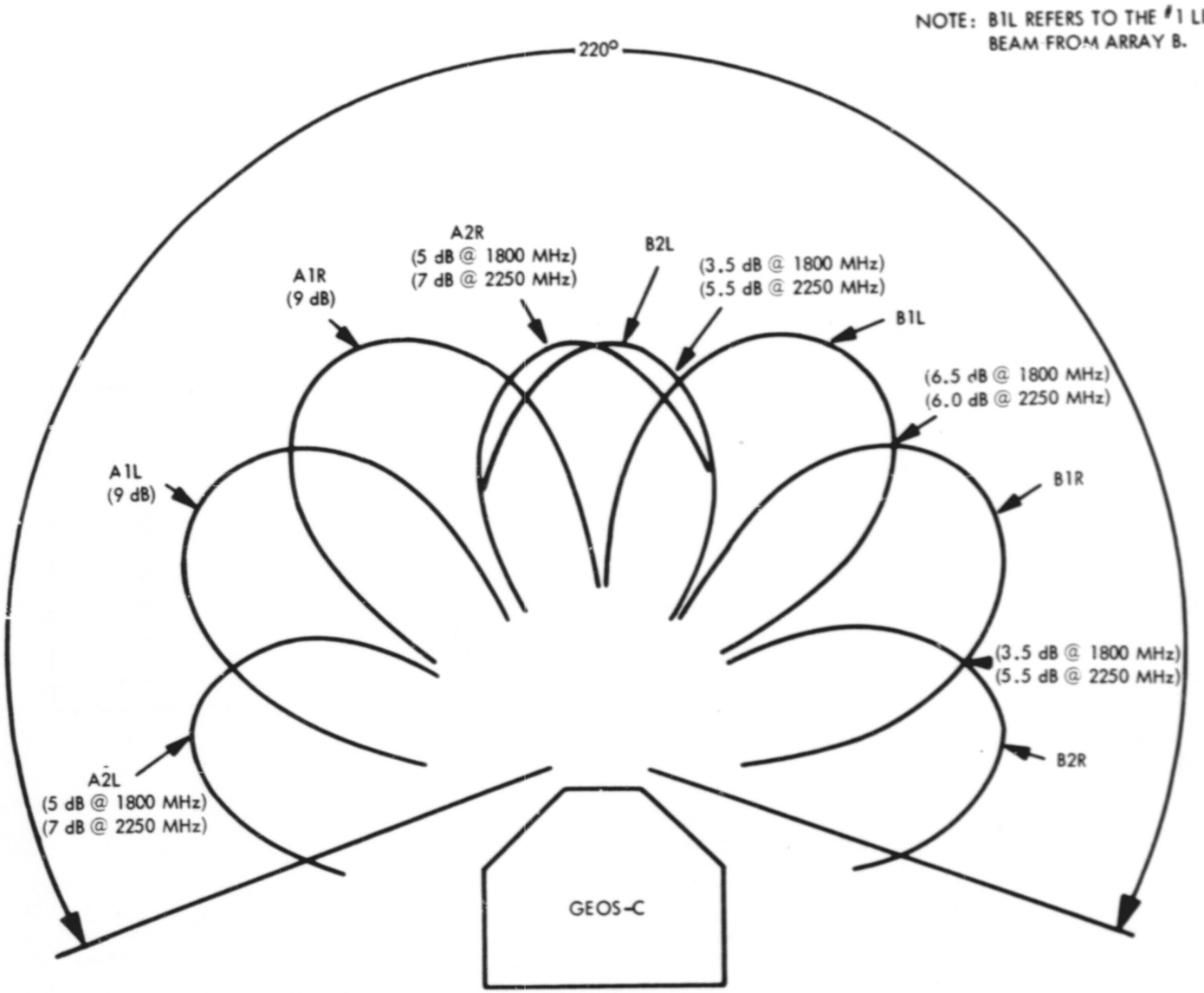

Figure 6-8. Antenna Beams for Electronically Steerable Arrays

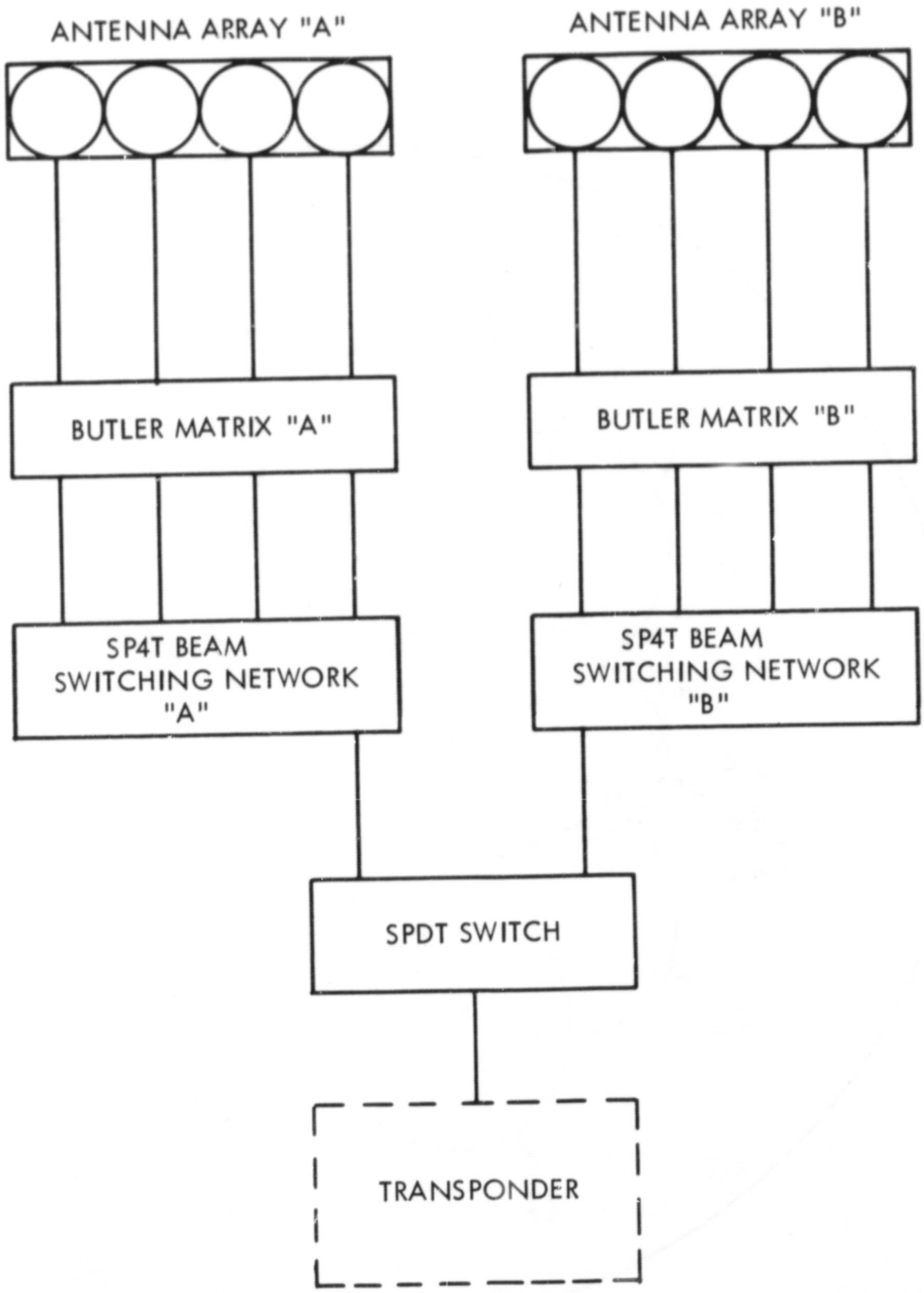

Figure 6-9. Antenna System Block Diagram for Electronically Steerable Arrays

Another possible approach would be to install one or two conical spiral antennas within the attach ring on GEOS-C. Conical spiral antennas for use with the GRARR S-Band transponder have been flown on GEOS-I and -II and on other spacecraft. This antenna is approximately 4 inches high and has a base diameter of 4 inches. Typically, antenna gain is greater than 0 dB relative to a circularly polarized isotropic antenna over approximately ±70 degrees from the antenna axis.

Vertical clearance for the 4 inch antenna height relative to the third stage motor used with GEOS-I and GEOS-II appears to be sufficient when using the presently available 8 inch high attachment fitting. However, access to the top of the third stage is required during pre-launch operations, and concurrence of cognizant launch vehicle personnel must be obtained. If use of the present attachment fitting proves to be unfeasible, a longer fitting could be used.

E. Range Tone Filtering Modification to GRARR Transponder

In attempting to improve the signal-to-noise power density ratio of the GRARR downlink sidebands and thereby improve system accuracy, when the input signal is weak, a range tone detection and filtering modification to the transponder were investigated. This modification had been investigated in the event a high gain antenna and/or a lower noise figure receiver was unattractive. The downlink frequency spectrum would be identical to that for the standard GRARR (see Appendix A), and multiple station tracking would be possible.

This method of transponder implementation was rejected for the following reasons:

Regeneration of small portions of the total ranging signal within any transponder has not been attempted to date. Delay variation between segments of the total ranging spectrum would cause range measurement difficulty, especially in ambiguity resolution.

Phase locked loop acquisition would be required.

Modification to the GRARR transponder would be significant. By using the standard GRARR transponder and newly developed power amplifier as planned for the NIMBUS-E spacecraft, cost and time saving will be realized.

Additional circuitry required for this modification is shown in Figure 6-10. The additional circuitry is placed between the post limiter filter

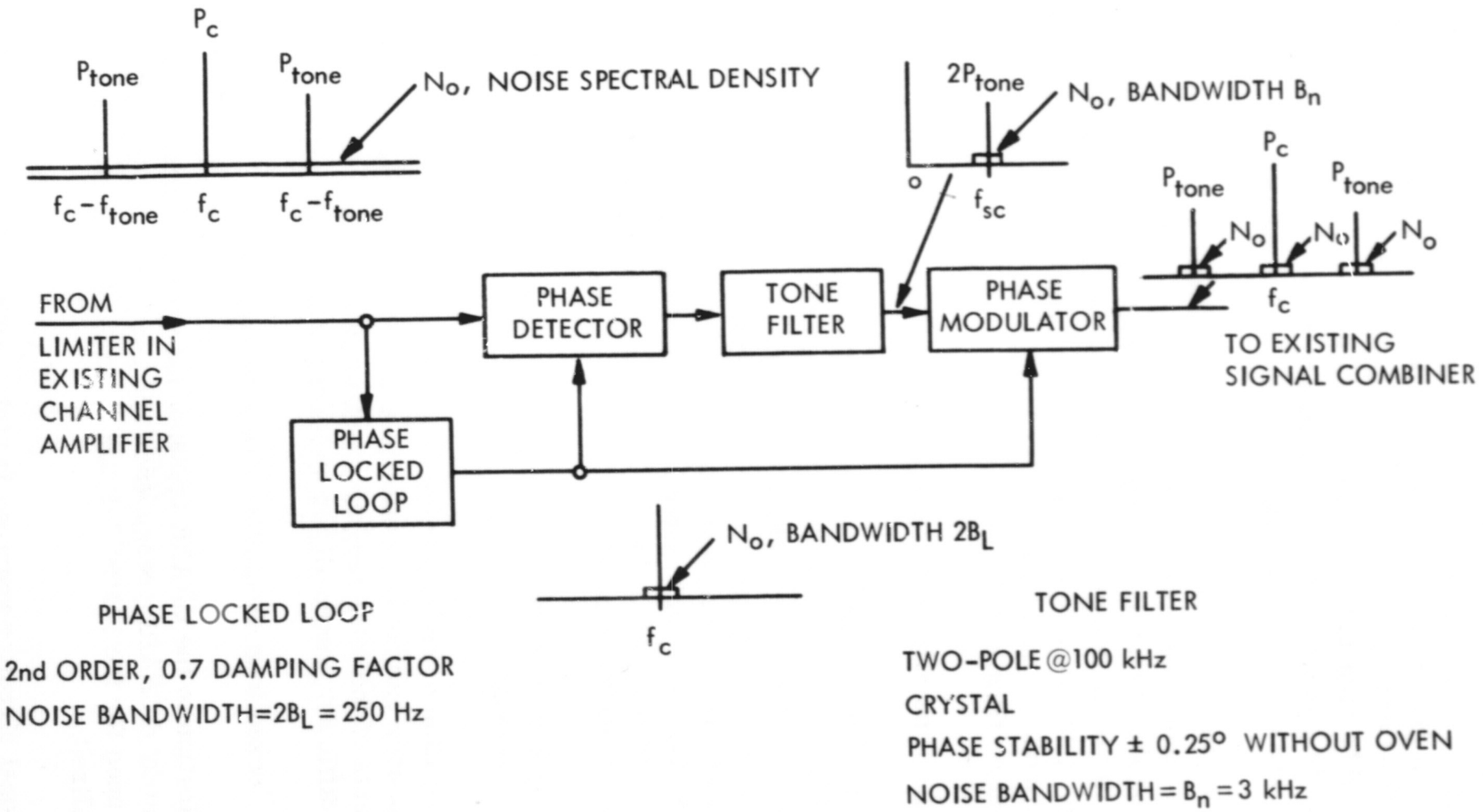

Figure 6-10. Range Tone Filtering Modification to GRARR Transponder

in the appropriate GRARR channel amplifier and the signal combiner which feeds the downlink phase modulator (refer to Figure A-1). The existing squelch gate would be replaced by an on-off command (as it also must be in the augmented GRARR transponder), otherwise the output of the new phase modulator will cause the transponder to transmit continuously. The purpose of the addition is to reduce the effective noise bandwidth of the channel used for tracking from ATS. It operates by tracking the carrier of the ATS signal, demodulating and filtering the range tone(s) and remodulating the carrier with the same modulation index. The spectra for a single range tone are shown on the figure. At the output of the modulator the signal is identical to that at the phase detector input with the exception that the noise appears only in the vicinity of the carrier and the two sidebands. The spectral density within the bandwidths of tracking and tone filters is ideally the same as at the input to the phase demodulator.

The bandwidth of the tone filter must be narrow enough to ensure that the remodulated ATS signal to noise ratio into the downlink modulator is high enough so that the signal achieves essentially all of the modulation index. On the other hand, it must be wide and stable enough to result in adequate tone phase stability over the desired environment. Reduction in bandwidth below that required to effectively "clean up" the modulated ATS signal is not effective since the re-radiated noise spectral density received at the ATS remains essentially constant for bandwidths below this value. A conservative 3 kHz was used for the tone filter noise bandwidth (a margin to allow for the small loop filter contribution is included). This results in a remodulated signal to noise ratio of 14 dB when a 0 dB gain antenna and a 1200°K receiving system noise temperature is used. This is a seeming improvement of approximately 25 dB over the standard GRARR transponder (2×550 kHz/3 kHz) except that the limiting factor here is ground system resolution, if it is assumed that a suitable transponder could be built.

Parametric analyses were performed for the same transmitter power (P) and antenna gain (G) values as in the augmented transponder analysis in Section B. Since the alternate approach would probably be preferred only if a receiver with a lower noise temperature could not be implemented, only a 1200°K noise temperature was considered.

Range and range rate errors are listed in Table 6-6 for the same operational modes as in Section B; that is:

Single channel tracking

Range error (σ_R)

Range tone = 100 kHz
Tracking bandwidth = 1 Hz

Range rate error ($\sigma_{\dot{R}}$)

No range tone

Tracking bandwidth = 2 kHz (B_n = 1 kHz)

Sampling rate = 1/second

TABLE 6-6

Range and Range Rate Errors—
Range Tone Filtering Modification

T (°K)	Parameters G(dB)	P (W)	σ_R (meters)	$\sigma_{\dot{R}}$ (meters/sec)
1200	0	1	5.0	.041
		4	3.4	.026
		10	3.0	.021
	3	1	3.9	.030
		4	2.8	.020
		10	2.5	.016
	6	1	3.1	.022
		4	2.5	.016
		10	2.3	.013
	9	1	2.6	.017
		4	2.4	.013
		10	2.3	.012

A brief investigation has shown that carrier acquisition and tracking of the phase locked loop does not present a problem. An example which illustrates the feasibility of the approach is presented in the following paragraphs. Maximum doppler frequency and rate will be 44 kHz and 47 Hz/second, respectively, for a nominal uplink carrier frequency of 1800 MHz.

Consider a transponder carrier tracking loop noise bandwidth ($2B_L$) of 250 Hz. This was chosen as a first order compromise between carrier acquisition, static and dynamic tracking considerations, contribution to noise bandwidth of the modified transponder, and adequate rejection of the 4 kHz range tone. The total received worst case power to noise density (including a 1 dB limiter suppression) into the loop is 44.7 dB - Hz for a 0 dB gain antenna and a 1200°K system noise temperature. If dual tone modulation is used, the carrier component is down 3.7 dB to 41 dB - Hz. The signal to noise ratio in the loop after acquisition is therefore

$$(S/N)_{2B_L} = 41 - 24 = 17 \text{ dB}$$

which is much more than adequate for carrier tracking. During acquisition the range tones will be shut off at the tracking station (standard practice) until all loops in the system lock. This prevents lockup on any spectral component but the carrier, and provides even higher S/N for acquisition. These values result in essentially noiseless acquisition.

The loop natural frequency, ω_n, (for a 0.707 damped loop) is 236 rad/sec which results in a maximum sweep rate for "assured" acquisition of

$$\Delta\dot{\omega} = \frac{\omega_n^2}{2} = 2.8 \times 10^4 \text{ rad/sec}^2$$

The maximum carrier acquisition time assuming totally unknown location in the assumed uncertainty band of ±50 kHz is

$$\tau = \frac{\Delta\omega}{\Delta\dot{\omega}} = 23 \text{ secs}$$

The dynamic phase lag for the worst case doppler rate of 50 Hz/sec will be

$$\theta_a = \frac{\Delta\dot{\omega}}{\omega_n^2} = 0.005 \text{ radians}$$

which is negligible.

The acquisition time indicated is an absolute maximum. Considerable improvement may occur most of the time. If, for example, GEOS is acquired as it rises above the ATS horizon, the doppler is near maximum and is the major component of frequency uncertainty. The doppler rate is negligible compared to the allowable VCO sweep rate. If the loop VCO is programmed to search from the high side of the uncertainty band, acquisition should occur in a few seconds at most. Other possibilities can be postulated such as commanding the sweep start point and direction.

F. Modified SGLS Transponder

A second backup approach was also investigated. This approach uses a portion of the transponder developed under the SGLS Program. A block diagram is shown in Figure 6-11. Operation is similar to the modified GRARR transponder in that the incoming signal is coherently demodulated using a phase locked detector. The entire range tone spectrum is filtered (this is in contrast to the rejected approach in Section E, wherein each significant spectral component is separately filtered) to reduce the noise bandwidth and is phase modulated on a carrier coherently derived from the tracked input carrier. The main difference, and advantage over the modified GRARR transponder described in Section E is that the range tones appear as singly modulated rather than doubly modulated sidebands and thus incur less modulation loss.

This type of tracking relay experiment transponder was rejected for the following reasons:

Two channel or simultaneous tracking (ground/GEOS-C, and ATS-F/GEOS-C) is not feasible unless two transponders are provided

Phase locked acquisition would be required

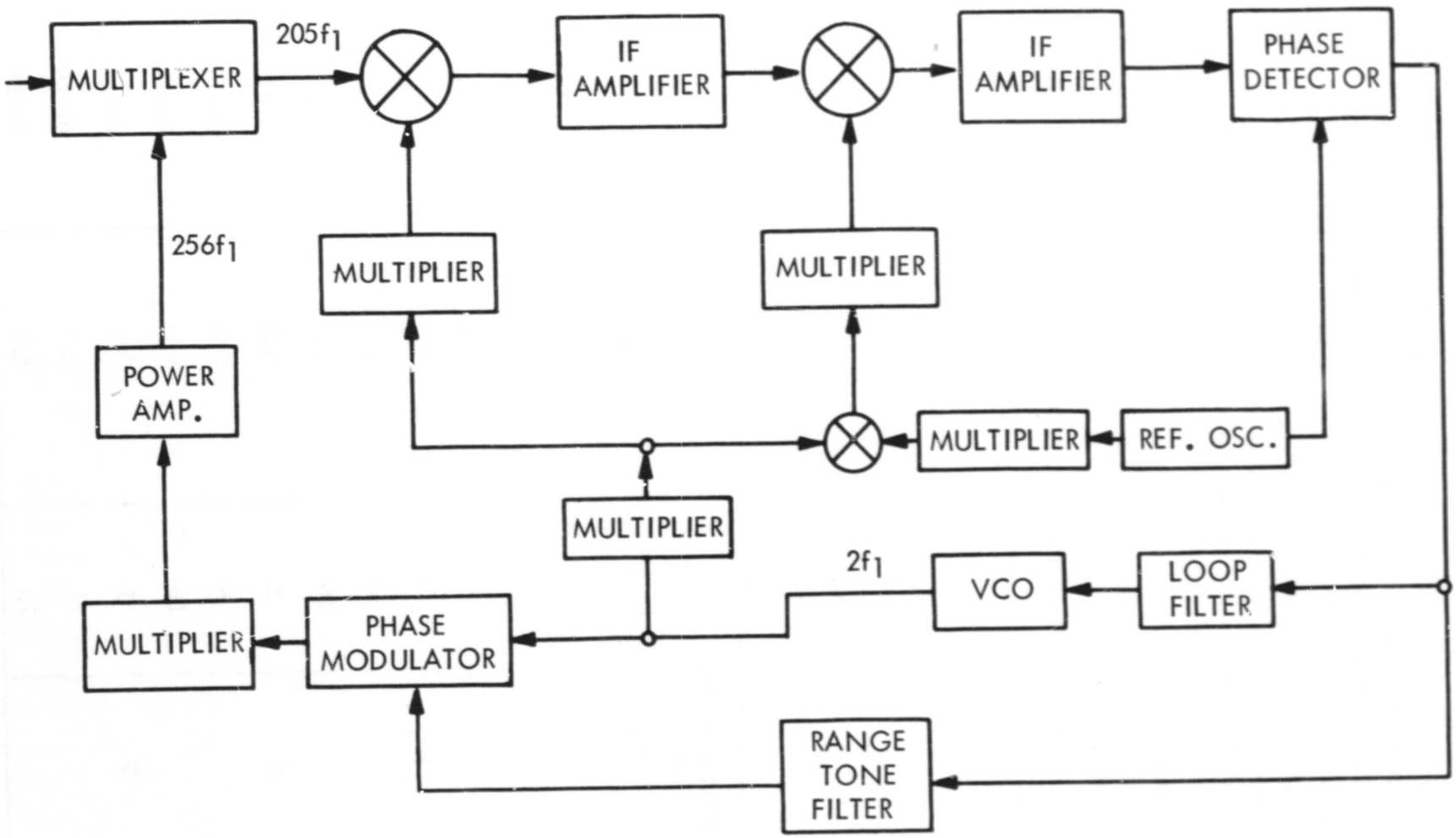

Figure 6-11. Modified SGLS Transponder

As shown in Appendix D, under strong signal conditions, noise limited range rate performance is improved by about a factor of 3 relative to the modified transponder. Range rate tracking performance of this alternative can therefore be approximated by dividing the error due to thermal noise of the modified transponder by 3 and calculating the root-sum-square of this value with the resolution error. (Changes in re-radiated noise from the transponder will lower the improvement factor slightly.) Resolution error at 1 1/sec sample rate is assumed to be approximately 0.01 meters/second as for the standard GRARR system. Under the conditions chosen in Section E, range tracking performance is identical to that of the modified GRARR transponders. Calculated values of range error and range rate error are listed in Table 6-7.

TABLE 6-7

Range and Range Rate Errors–
Modified SGLS Transponder

Parameters				
T (°K)	G (dB)	P (W)	σ_R (meters)	$\sigma_{\dot{R}}$ (meters/sec)
1200	0	1	5.0	0.017
		4	3.4	0.013
		10	3.0	0.012
	3	1	3.9	0.014
		4	2.8	0.012
		10	2.5	0.011
	6	1	3.1	0.012
		4	2.5	0.011
		10	2.3	0.011
	9	1	2.6	0.011
		4	2.4	0.010
		10	2.3	0.010

G. Range and Range Rate Accuracy Comparison

Calculated values of range error for the proposed and rejected approaches are presented in Figure 6-12. The values reflect single channel tracking, 100 kHz range tone and 1 Hz tracking bandwidth operational considerations. The curves are based on a 1200°K input noise temperature for each transponder, and points are plotted for 600°K and 6 dB gain for the augmented GRARR transponder. Calculated values of range rate error are plotted in Figure 6-13 for single channel tracking, no range tone, tracking bandwidth B_n = 1 kHz, and 1/second sampling rate.

Examination of the curves indicates that the accuracy of the augmented GRARR transponder (the intended choice) having an input noise temperature (T) of 1200°K, antenna gain (G) of 6 dB, and output power (P) of 4 watts approaches the resolution of the GRARR system. Actually, accuracy is less than twice system resolution. Decreasing T to 600°K or increasing P to 10 watts improves the accuracy, but the improvement is not substantial because of the system resolution limitation. Comparable accuracy can be obtained with G = 3 dB, T = 600°K and P = 10 watts.

The accuracy of the modified GRARR transponder (with range tone filtering) with T = 1200°K, G = 3 dB and P = 4 watts will be less than twice system resolution in range and approximately twice system resolution in range rate. Increasing P to 10 watts improves range rate accuracy by 20 percent from 0.020 to 0.016 meters/second.

Use of a modified SGLS transponder with T = 1200°K, G = 0 dB and P = 4 watts will result in a system accuracy which approaches system resolution. Increasing P to 10 watts improves the accuracy by approximately 10 percent, but decreasing P to 1 watt will degrade range accuracy to more than twice system resolution.

H. Conclusions

The development of a GEOS-C/ATS-F tracking experiment which will yield data of geodetic precision is feasible. Weight, volume and power requirements will have little, if any, impact on the GEOS-C design. Modification of the ATS-F spacecraft will not be required.

The proposed approach to spacecraft hardware implementation is: Standard GRARR transponder augmented with a low noise input circuit and an output power amplifier, and an antenna having a 6 dB gain.

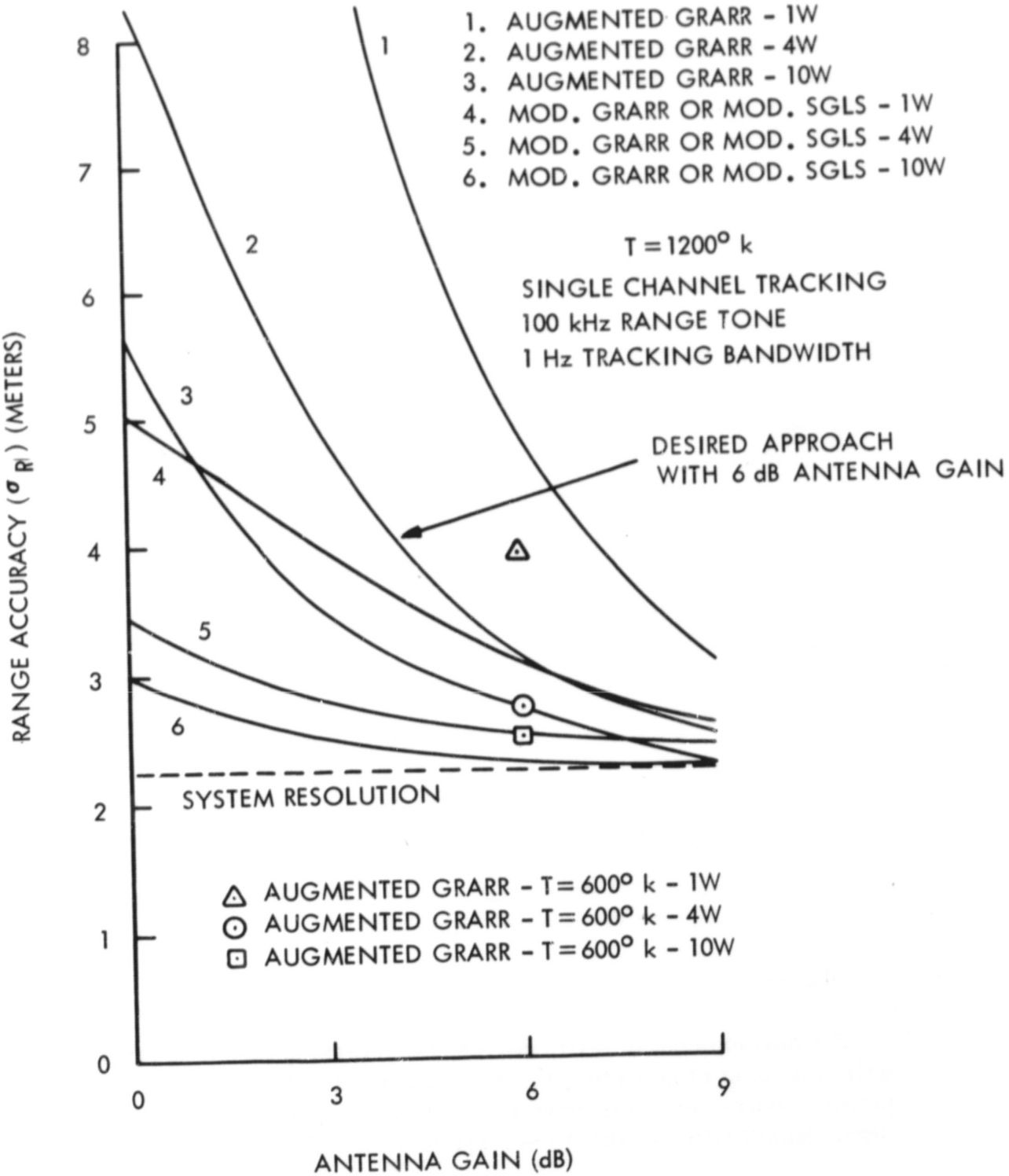

Figure 6-12. Range Accuracy Comparison

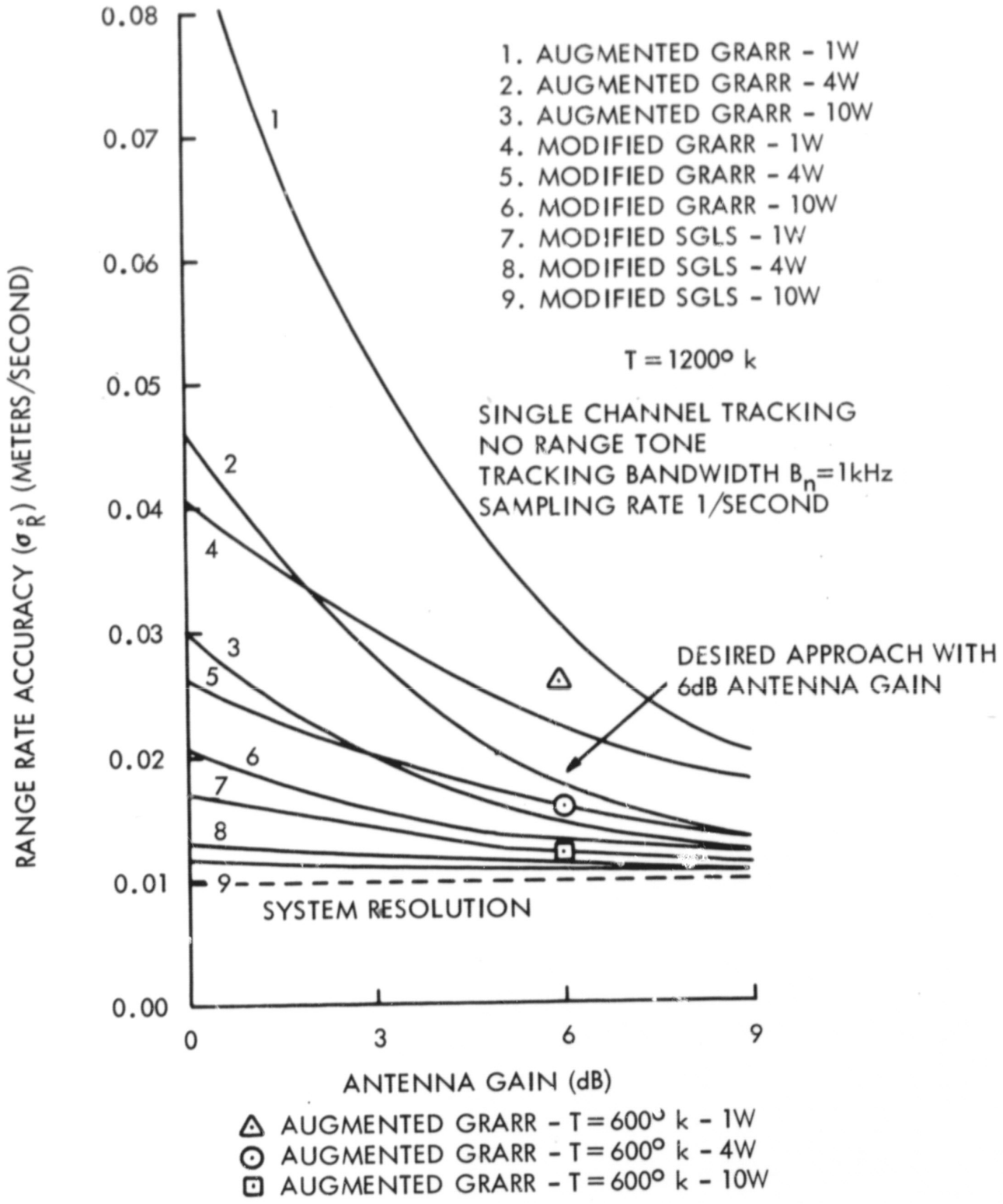

Figure 6-13. Range Rate Accuracy Comparison

The rejected approaches are:

1. A modified GRARR transponder with range tone filtering in one channel, a RF output power amplifier, and a low gain antenna. This approach would have required design of a phase locked loop and extremely stable range tone filter circuitry for the applicable tracking channel in the transponder.

2. A phase locked loop transponder with a RF output power amplifier and a low gain antenna. Basically, a Unified S-Band transponder utilizing Space Ground Link System frequencies and modules had been proposed. No advantage in range measurement would have accrued with the disadvantages of phase locked operation.

VII. DATA MEASUREMENT REQUIREMENTS

A. GEOS-C/ATS-F Tracking Data

1. Geodetic Purposes

To utilize the tracking data for geodetic purposes, it would be advantageous to have ATS-F track GEOS-C continuously over half-orbit passes of GEOS-C. A set of possible tracking schemes has already been outlined in Section IV, B, 2.

2. Orbit Determination

For orbit determination, GEOS-C/ATS-F tracking data would be needed for each GEOS-C pass over a prescribed period of time. For example, for a 24-hour period, one possible scheme would be to track GEOS-C over three, 3-min. periods per each GEOS-C pass.

VIII. OPERATIONAL REQUIREMENTS

A. Ground Station Requirements

As in the NIMBUS-E/ATS-F Data Relay Experiment, one fixed ATS Ground Station will be used to transmit and receive the tracking signals to and from ATS-F. In addition a Mobile ATS Ground Station will be used to simulate GEOS-C on the ground and will function as a test target for the orbiting ATS-F prior to ATS-F operation with GEOS-C.

GRARR stations also will track the GEOS-C spacecraft directly as for the previous GEOS I and GEOS II missions, but with the additional capability of simultaneously tracking with ATS-F when mutual visibilities exist. GEOS-C will also carry an APOLLO USB transponder so that the 14 MSFN stations can participate in the precision tracking of GEOS-C. Of the five GRARR sites, only Alaska will not have visibility of an orbit inclined at 20°. All 14 MSFN stations will have visibility.

The ATS-F equipment at the ATS Ground Stations must be modified to permit extraction of range-rate information from the carrier and 2.4 MHz subcarrier (derived from uplink carrier) transmitted from the GEOS-C GRARR transponder via ATS-F. This modification (entitled the ATS-R Receiver Modification Unit) is discussed in Reference 3. The ATS Project Office is funding the construction and installation of this unit for the NIMBUS-E/ATS-F Data Relay Experiment. It is fully compatible with the proposed GEOS-C spacecraft equipment and it is assumed to be available for this experiment

For investigation of range rate tracking data improvement to 0.1 millimeter per second, it will be necessary to extend the ground tracking system measurement interval from its maximum value of approximately 6 seconds to as large as 50 seconds. For the theoretical advantage of long measurement intervals, or correspondingly a number of contiguous, correlated, shorter measurements, see Reference 9. To instrument this capability in the ground tracking system, it will be necessary to make one minor change to the Doppler measurement process beyond the modifications planned for the NIMBUS-E/ATS-F experiment. Figure 8-1 presents a function description of the planned NIMBUS-E/ATS-F Doppler measurement. With this method a time interval is measured and this time interval represents the time required to count or accumulate "N" (a fixed number) cycles of Doppler plus bias frequency. The time interval unit and the N-cycle counter are reset at the sample rate.

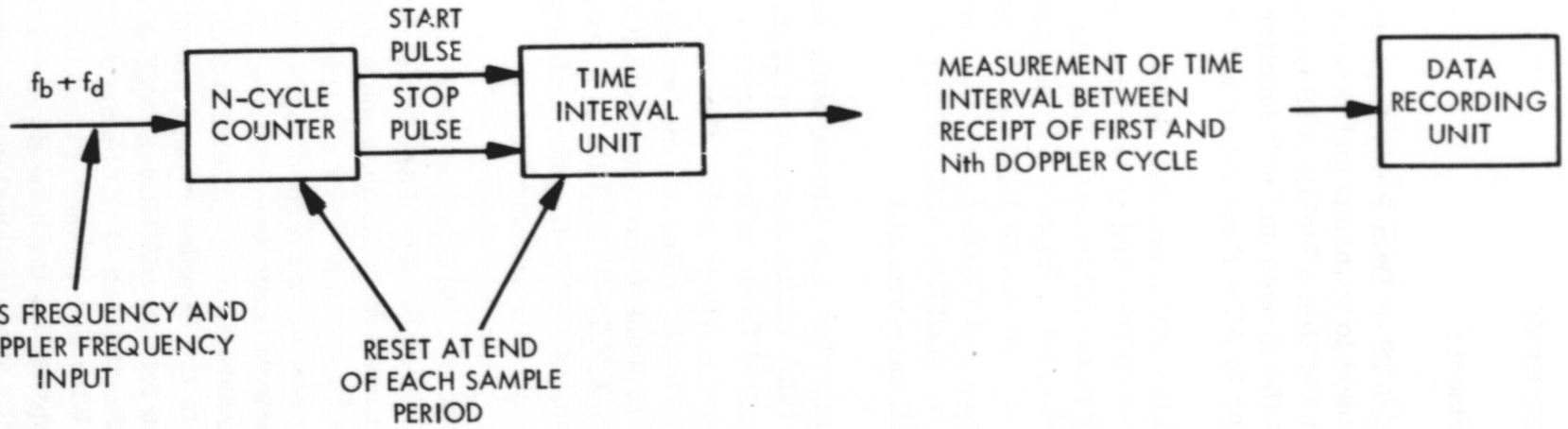

Figure 8-1. Method of Doppler Measurement, ATS-F/NIMBUS-E

For the GEOS-C tracking experiment, the required Doppler counting is shown in Figure 8-2. The T-cycle counter registers the continuous count of Doppler and bias cycles and the data recording unit samples the contents of the T-counter non-destructively (no reset) at the data sample rate.

The magnitude of the required equipment change is as follows:

Provide a means of switching the $f_b + f_a$ input to either the N-cycle counter or the time interval unit. The present time interval unit is adequate for use as the T-cycle counter.

Provide a means of sampling the T-counter registers at the sample rate.

Data recording and data format will remain unchanged.

The present data recording and data formatting provide for 8 digits of data. It can be calculated that the read-out capacity of the T-counter will be exceeded every 170 seconds at the worst.

To minimize changes to the data formatter and recorder, ambiguities in the total Doppler count will most easily be removed by the automated preprocessing of the raw data prior to the orbit determination program.

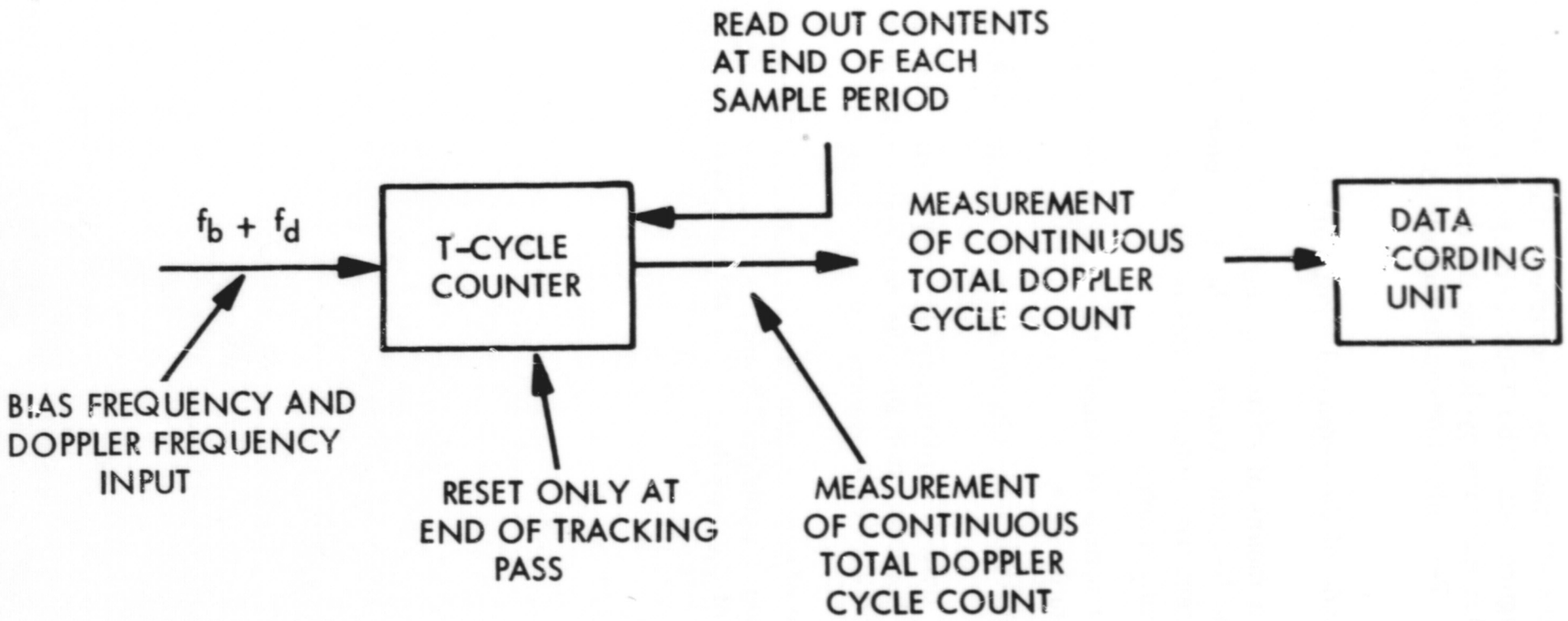

Figure 8-2. Required Method of Doppler Measurement, ATS-F/GEOS-C

REFERENCES

1. "Proposed Earth Physics and Geodesy Programs Including an ATS-GEOS Tracking and Orbit Determination Experiment," letter from J. W. Siry to NASA Headquarters, J. Naugle and J. Rosenberg, with enclosure, August 27, 1969.

2. "Tracking and Communications for Planetary Manned Mission," F. O. Vonbun and J. T. Mengel, Journal of Spacecraft and Rockets, Vol. 5, No. 7, July 1968, pp. 863-865.

3. "ATS-F/NIMBUS-E Data Relay Experiment Technical Summary," GSFC DR 1-0000, dated October 1968, Rev. B.

4. "Proposal for the Development of NIMBUS Flight Hardware for the NIMBUS-ATS Data Relay and Tracking Experiment RF and Digital Electronics," dated October 23, 1969, prepared by GSFC, Space Electronics Branch, Code 562.

5. "The Interface between Satellite Altimetry and Orbit Determination," C. A. Lundquist, presented at the 3rd Seminar on Guidance and Trajectory Analysis of the Electronics Research Center (NASA), May 31-June 1, 1967.

6. "Orbital Error Studies--Tracking from a Synchronous Spacecraft," J. L. Cooley and A. Marlow, GSFC X-551-69-7, January 1969.

7. "Space Trajectories and Errors in Time Frequency and Tracking Station Location," F. O. Vonbun, GSFC X-507-67-163, April 1967.

8. "ATS Orbit Determination Accuracy for Various Tracking Configurations," R. H. Green, IBM Report No. TM 68-40 for NASA Contract No. NAS 5-10022, October 1968.

9. "Effects of Correlated Noise with Applications to Apollo Tracking Problems," B. Kruger, NASA TN D-4121, February 1968.

10. "GRARR Design Evaluation Report," General Dynamics Report R-67-042, dated December 13, 1967, prepared for GSFC under Contract No. NAS 5-10555.

11. "GRARR S-Band Transponder Specifications," GSFC Spec. S-530-P-2, January 1967.

12. "Analysis of Signal and Noise Turnaround in the Goddard Range and Range Rate Transponder," T. L. Grenchik, GSFC X-551-69-323, August 1969.

13. "Tracking ATS by Lasers," Memorandum of January 30, 1970, Mrs. A. Marlow to Dr. F. O. Vonbun.

14. "GEOS-C/ATS-F Tracking and Orbit Determination Experiment," by Communications and Systems, Inc., The Johns Hopkins University/Applied Physics Laboratory, and Goddard Space Flight Center.

APPENDIX A

GODDARD RANGE AND RANGE RATE SYSTEM

The Goddard Range and Range Rate (GRARR) system typically consists of one or more ground tracking stations and a spaceborne transponder. Typical ground station power output ranges from 1 to 10 kilowatts, and the steerable ground tracking antennas have beamwidths of approximately 3 degrees. Polarization of the radio frequency energy is either right-hand or left-hand circular. The spacecraft antenna, usually a fixed conical spiral, accepts the RF energy and sends it to the transponder where it is converted and retransmitted through the same antenna to the same ground station. Capability exists for tracking from one, two or three ground stations simultaneously.

The frequency of the carrier transmitted by the ground station is 1799.2, 1800.0 or 1801.0 MHz. Available ranging tones, which are phase modulated on the carrier, are:

8 Hz	4 kHz
32 Hz	20 kHz
160 Hz	100 kHz
800 Hz	500 kHz

Any one of the three highest tones may be selected and is transmitted continuously. Each lower tone is sequentially applied one at a time with the highest tone selected to resolve range ambiguities (Reference A-1). The lowest four tones are complemented with a 4 kHz tone so that modulation products are not near the carrier frequency. Therefore, the actual modulation frequencies corresponding to the four lowest tones are 4.8, 4.16, 4.032 and 4.008 kHz.

A block diagram of the GRARR transponder is shown in Figure A-1 (Reference A-2). The crystal oscillator frequency of 37.55 MHz is multiplied by 49 to obtain a frequency of 1839.95 for mixing with the incoming signal. After amplification in the IF amplifier, the oscillator frequency is again mixed with the 37.55 MHz crystal oscillator to obtain one or more frequencies corresponding to the center frequencies of the filters. The input, IF, and filter frequencies are listed in Table A-1. Therefore, the information transmitted by a ground station passes through one of the three narrow band filters depending on the frequency of the carrier transmitted by the ground station, and the transponder can process signals from three ground stations simultaneously.

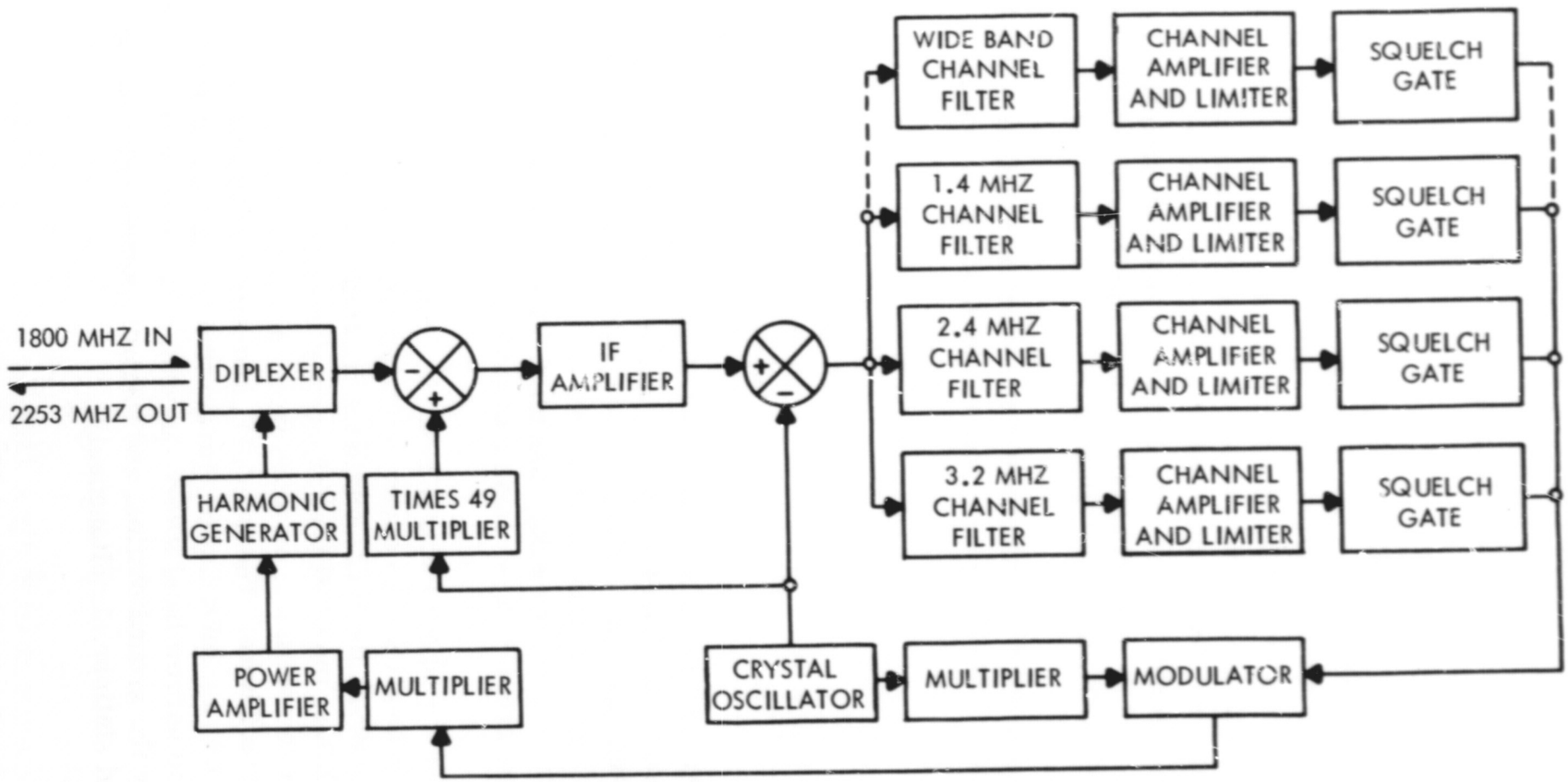

Figure A-1. Block Diagram, GRARR S-Band Transponder

(Reference A-2)

Table A-1

GRARR Transponder Frequencies (MHz)

Input	IF (1839.95—Input)	Filter (IF—37.55)
1799.2	40.75	3.2
1800.2	39.95	2.4
1801.0	38.95	1.4

The channel filters have noise bandwidths of 550 kHz for each of the three narrowband channels and 3.9 MHz for the wideband channel. Center frequency of the optional wideband channel* is 2.4 MHz which corresponds to the 1800.0 MHz uplink carrier, and this is the only filter which will pass the highest ranging tone of 500 kHz.

The output of the filters is limited and phase modulated on a multiple of the oscillator frequency, and this phase modulated signal is again multiplied so that the transmitted carrier is 60 times the oscillator frequency or 2253.0 MHz. Modulation components, or subcarriers, are centered at ±1.4, 2.4, and 3.2 MHz relative to the carrier depending on the frequency transmitted by the ground station as shown in Table A-1, and the ranging tones are arranged around the respective subcarriers. A typical output frequency spectrum is shown in Figure A-2. The downlink carrier frequency includes transponder oscillator instability and oneway doppler shift, while the spacing of the modulation components relative to the carrier include oscillator instability and two-way doppler. Therefore, oscillator instability can be separated from the frequency shift due to vehicle velocity. Transmitter output power is nominally 1 watt, but may be tailored according to the mission to 1/4, 1/2, 3/4, 2, or 10 watts.

REFERENCES

A-1 "GRARR Design Evaluation Report," General Dynamics Report R-67-042 dated 13 December 1967, prepared for GSFC under Contract No. NAS 5-10555.

A-2 "GRARR S-Band Transponder Specifications," GSFC Spec S-530-P-2, January 1967.

*Wideband channel operation cannot occur simultaneously with narrowband operation.

Figure A-2. Typical GRARR Transponder Output Frequency Spectrum

APPENDIX B

RANGE AND RANGE RATE ERRORS—

AUGMENTED GRARR TRANSPONDER

Errors in the range and range rate measurements for the GEOS-C/ATS-F tracking experiment are listed for the indicated values of GRARR transponder input noise temperature (T), antenna gain (G) and RF output power (P). Calculations are discussed in Section B. The ground tracking station is assumed to be operating in the following mode:

Single channel tracking

Range error (σ_R)

Range tone = 100 kHz

Tracking bandwidth = 1 Hz

Range rate error ($\sigma_{\dot{R}}$)

No range tone

Tracking bandwidth = 2 kHz (B_n = 1 KHz)

Sampling rate = 1/second

In this operating configuration system resolution is 2.23 meters in range and 0.00975 meters/second in range rate.

T (°K)	G (dB)	P (W)	σ_R (meters)	$\sigma_{\dot{R}}$ (meters/sec)	Sample rate
1200	0	1	17.0	0.089	1/sec
		4	8.3	0.046	
		10	5.5	0.030	
	3	1	9.4	0.052	
		4	4.8	0.028	
		10	3.4	0.020	
	6	1	4.8	0.030	
		4	3.1	0.017	
		10	2.7	0.014	
	9	1	3.1	0.020	
		4	2.5	0.013	
		10	2.3	0.012	
600	0	1	13.0	0.073	
		4	6.8	0.037	
		10	4.6	0.025	
	3	1	6.8	0.041	
		4	3.8	0.023	
		10	2.9	0.016	
	6	1	3.9	0.026	
		4	2.7	0.016	← proposed approach
		10	2.5	0.012	
	9	1	2.9	0.018	
		4	2.4	0.012	
		10	2.3	0.011	
300	0	1	9.0	0.057	
		4	4.8	0.030	
		10	3.4	0.021	
	3	1	4.8	0.035	
		4	3.1	0.020	
		10	2.7	0.015	
	6	1	3.4	0.025	
		4	2.7	0.015	
		10	2.3	0.013	
	9	1	2.8	0.018	
		4	2.3	0.013	
		10	2.3	0.011	

APPENDIX C

COMPONENTS OF ELECTRONICALLY STEERABLE ANTENNA ARRAY

This appendix contains descriptions of the various blocks of the electronically steerable arrays shown in Figure 6-5.

ANTENNA ELEMENTS

Each of the eight antenna elements consists of a metallic Archimedean spiral printed on dielectric board. Figure C-1 shows the spiral mounted in a cylindrical cavity. The spiral is flush-mounted on the GEOS slant face to prevent solar cell shadowing. Each antenna is three inches in diameter by two inches deep. The antennas are fed by a coaxial input on the rear cavity wall. A printed circuit balun transforms the unbalanced coaxial input to a balanced feed at the spiral center terminals. The balun is mounted on a printed circuit board along the cavity centerline as shown in Figure C-1. The spiral antenna has an axial ratio less than 2.0 dB and a gain of 6 dB above circular isotropic. Each antenna has a weight of 90 grams. Half-power beamwidth is 70 degrees for each element. The elements are spaced on three-inch centers.

BUTLER MATRIX

Each of the two Butler matrices consists of a low-loss power divider and phasing system for four antenna elements. Figure C-2 shows a Butler matrix consisting of four 90-degree hybrid couplers 1L, 2L, 1R, 2R and four output ports labelled 1, 2, 3, 4 which connect to the antennas. When a signal is applied to one of the input ports, the matrix divides the power equally amoung the output ports 1, 2, 3, and 4 with the proper phase gradient to steer the antenna beam. Each input port of the Butler matrix provides a different phase gradient across the output ports so that overlapping anterna beams can be generated by the array.

The matrix insertion loss is 0.5 dB and each matrix weighs 0.42 pounds.

BEAM SWITCHING NETWORK

Each of the two beam switching networks consists of a single-pole four-throw diode switch which connects the different beam ports of the Butler matrix to the matrix selection switch. The switching network is fabricated in stripline with an estimated weight of 0.2 pounds each. The switches will be impedance matched in the forward and reverse bias states with isolation of 25 dB and insertion loss of 0.5 dB. 100 milliwatts of drive power is required for the diode. The switch is shown in Figure C-3.

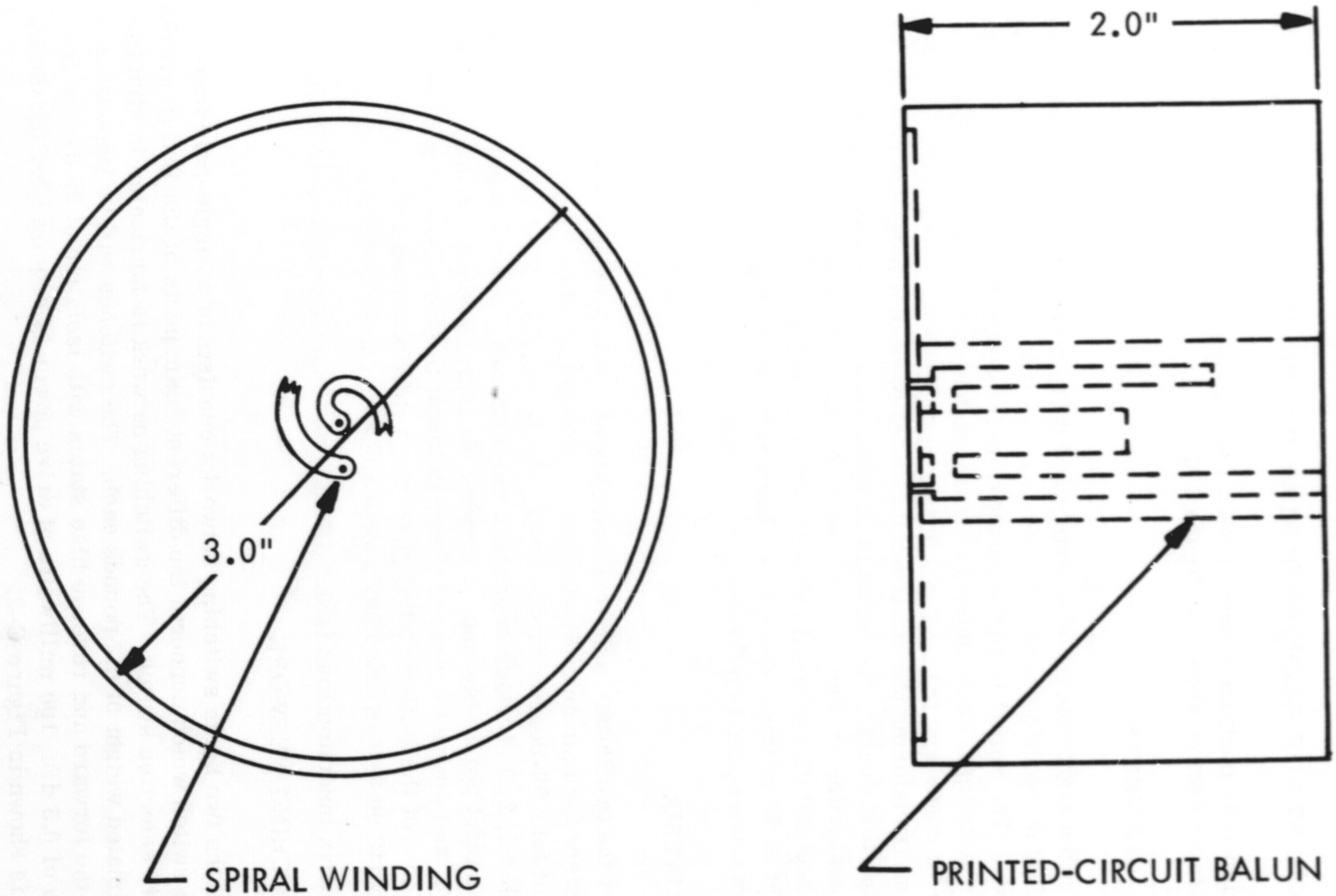

Figure C-1. Cavity-Backed Spiral Antenna

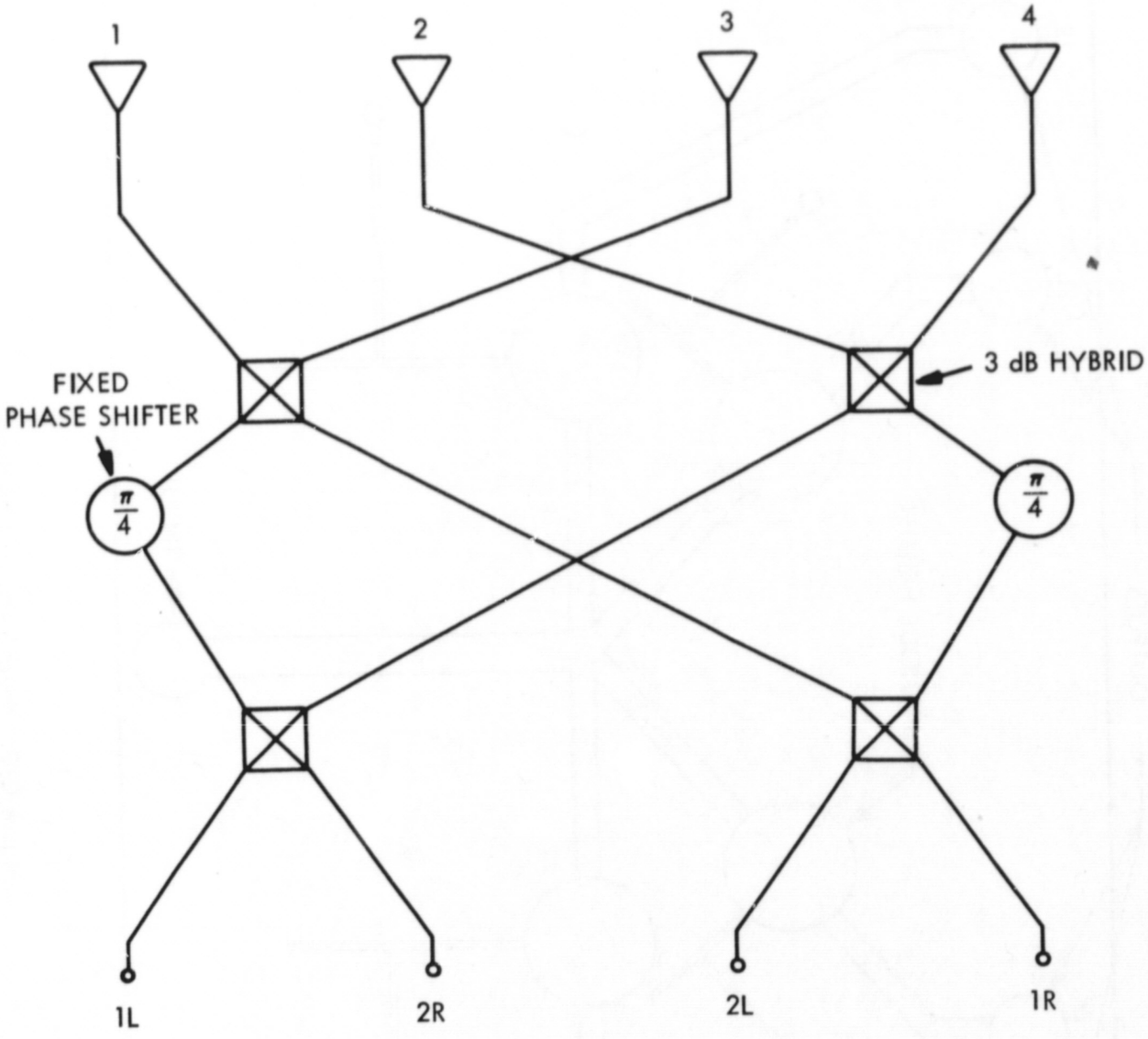

Figure C-2. Butler Matrix

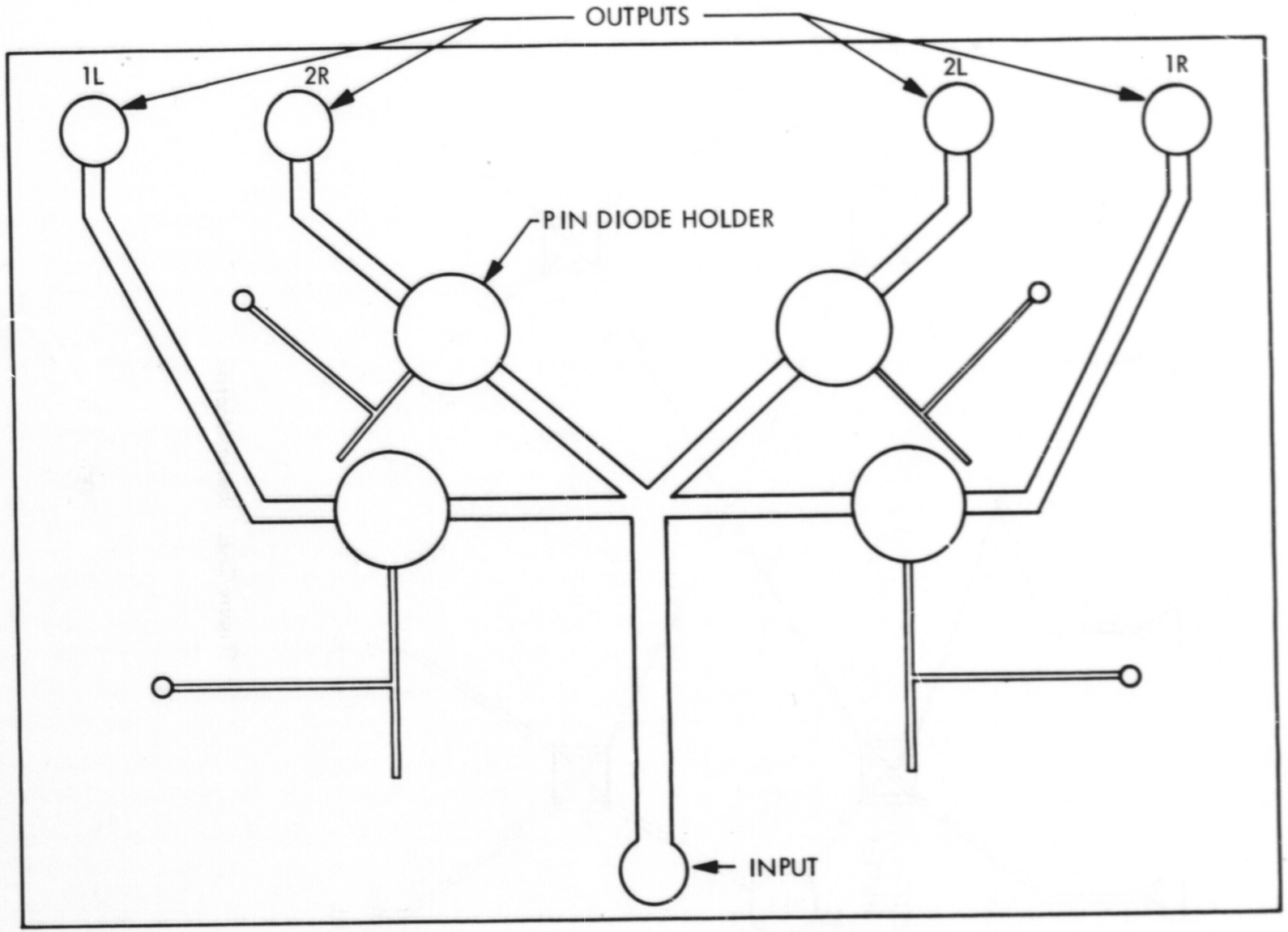

Figure C-3. Beam Switching Network

MATRIX SELECTION SWITCH

The inputs of the two beam switching networks are selected by a single-pole double-throw switch shown in Figure C-4. The switch consists of two diodes mounted in each branch arm of a tee. Insertion loss of the switch is 0.5 dB and isolation is 25 dB. The diodes will be impedance matched in the forward and reverse bias states. Estimated weight of the diode in a stripline configuration is 0.10 pounds. The DC power requirement is 100 milliwatts. The maximum RF power through the switch is three watts CW. Alternate diode configurations will be required for handling higher RF power levels.

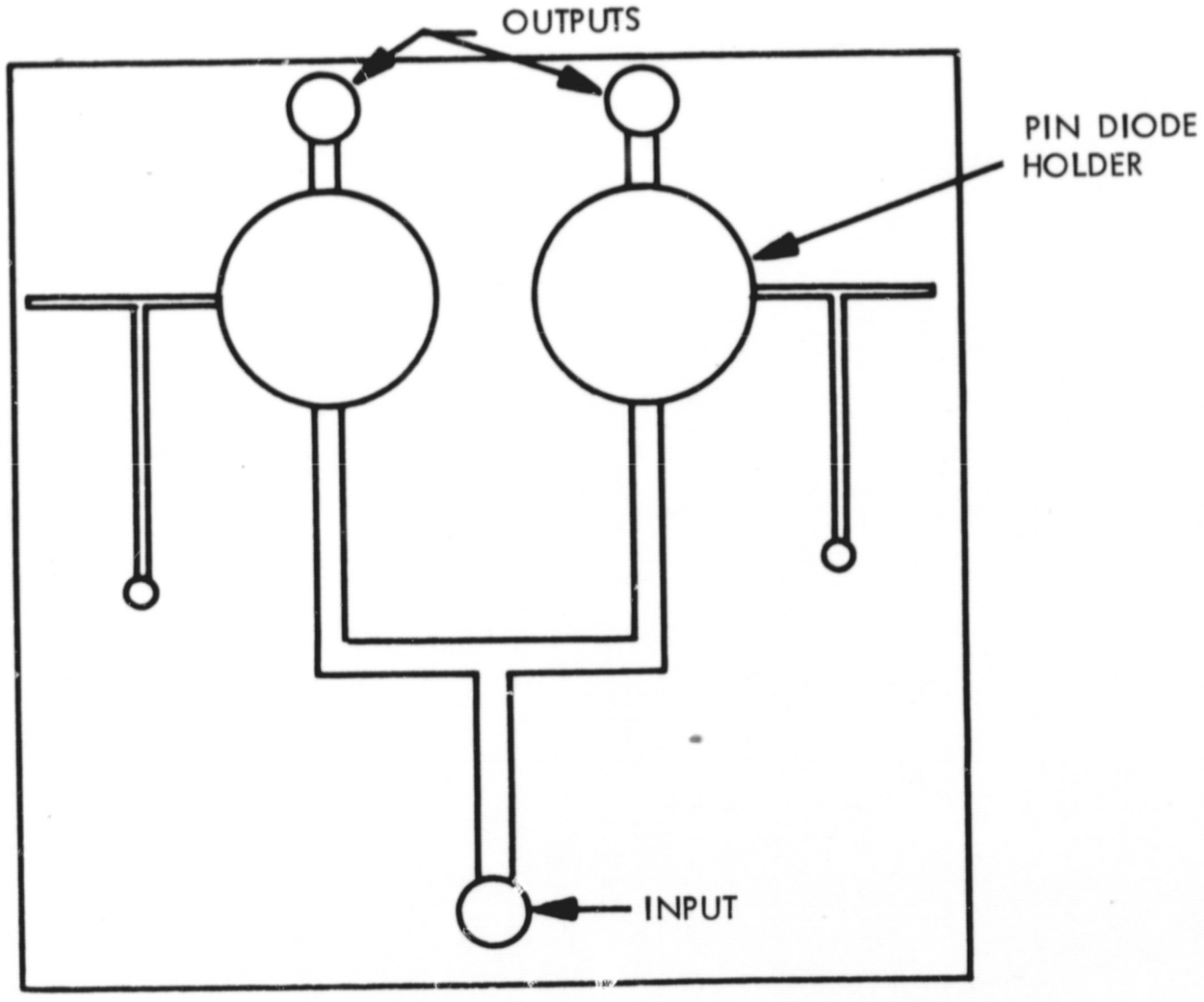

Figure C-4. Matrix A/B Switch

APPENDIX D

RANGE RATE PERFORMANCE OF GRARR AND SGLS TRANSPONDERS

The purpose of this Appendix is to compare the performances of the non-coherent GRARR and coherent SGLS transponders under high input signal conditions but when noise is the accuracy-limiting effect. Under these conditions, performance can be compared by considering the relative power in each of the signal spectral components for the same total transmitter power.

Consider first a single station tracking range-rate only. For the non-coherent GRARR transponder:

$$\sigma_{\dot{R}N} = K_N K_0 \left[\left(\frac{\phi}{S} \right)_{CN} + \left(\frac{\phi}{S} \right)_{SCN} \right]^{1/2}$$

where:

$\sigma_{\dot{R}N}$ = standard deviation in range-rate measurement.

$(\phi/S)_{CN}$ = noise density to carrier power.

$(\phi/S)_{SCN}$ = noise density to subcarrier power.

K_N = function of effective frequency on which doppler is measured.

K_0 = function of doppler bias frequency and doppler count smoothing interval.

If the total transmitter power is used as a reference and the GRARR modulation parameters are used:

$$\left(\frac{S}{\phi} \right)_{CN} = 0.263 \left(\frac{S}{\phi} \right)_T \qquad (5.8 \text{ dB down})$$

$$\left(\frac{S}{\phi} \right)_{SCN} = 0.616 \left(\frac{S}{\phi} \right)_T \qquad (2.1 \text{ dB down})$$

For the non-coherent GRARR transponder (and doppler processor), $K_N = \lambda_t/2$ (wavelength transmitted to transponder). K_0 is the same for coherent and non-coherent transponders.

Now, considering the coherent SGLS transponder, under the same tracking conditions:

$$\sigma_{\dot{R}C} = K_C K_0 \left[\left(\frac{\phi}{S}\right)_{CC}\right]^{1/2}$$

where $K_C = \lambda_t/2\rho$

ρ = turnaround ratio of the transponder

= $256/205 \approx 1.25$

$(\phi/S)_{CC}$ = noise density to carrier power

$(S/\phi)_{CC} = (S/\phi)_T$

Comparing the performance:

$$\frac{\sigma_{\dot{R}C}}{\sigma_{\dot{R}N}} = \frac{K_C}{K_N}\left[\frac{\left(\frac{\phi}{S}\right)_{CC}}{\left(\frac{\phi}{S}\right)_{CN} + \left(\frac{\phi}{S}\right)_{SCN}}\right]^{1/2} = \frac{1}{2.95}$$

If range tracking is done simultaneously using the highest tone only, the conditions for the non-coherent transponder are:

$$\left(\frac{S}{\phi}\right)_{CN} = 0.263 \left(\frac{S}{\phi}\right)_T \qquad (5.8 \text{ dB down})$$

$$\left(\frac{S}{\phi}\right)_{SCN} = 0.340 \left(\frac{S}{\phi}\right)_T \qquad (4.7 \text{ dB down})$$

$$\left(\frac{S}{\phi}\right)_{RN} = 0.258 \left(\frac{S}{\phi}\right)_T \qquad (\text{range tone } 5.9 \text{ dB down})$$

The modulation index for the coherent transponder will be chosen so that range tracking performance is the same, i.e.:

$$\left(\frac{S}{\phi}\right)_{RC} = 0.258 \left(\frac{S}{\phi}\right)_{T} \qquad \begin{pmatrix} 5.9 \text{ dB down results in} \\ \text{mod. index} = 0.77 \end{pmatrix}$$

and therefore

$$\left(\frac{S}{\phi}\right)_{CP} = 0.740 \left(\frac{S}{\phi}\right)_{T}$$

Comparing:

$$\frac{\sigma_{\dot{R}C}}{\sigma_{\dot{R}N}} = \frac{1}{2.82}$$

APPENDIX E

GRARR TRANSPONDER BENCH TESTS

Bench tests on a GRARR transponder were performed to determine the validity of the assumptions used to derive the curve of transponder output versus input at low input S/N shown in Figure 6-1. The tests were performed at the Goddard Space Flight Center using an Electrac Test set and the backup transponder for OGO-6. The transponder has the "B" wideband channel and the "C" narrowband channel. Tests were performed on the "C" channel. The test set output was first determined by comparing levels on a spectrum analyzer with a calibrated source at 1.8 GHz. The source calibration was also checked with a bolometer. The test set output, on channel C unmodulated, at the circulator output port, and with 10 dB of attenuation in the circulator input line, was -37.5 dBm. The attenuation between the circulator and the GRARR transponder was determined to be 53.5 dB, in both directions. This was done by feeding a measured +27 dBm in one end, and measuring -26.5 dBm at the other. Figure E-1 shows the test set up for measuring signal components out versus signal in. Measurements were performed by using a calibrated source to match output spectrum amplitudes on the spectrum analyzer.

Figure E-2 shows the measured values of the carrier and each of the two subcarriers. Differences in subcarrier levels are probably caused by nonlinearity of the transponder amplifier over the frequency range and are not considered to indicate a problem. Comparison with Figure 6-1, referencing 0 dB on Figure 6-1 to C_{in} = -106 dBm on Figure E-2, indicates that the curves are comparable.

The test set-up shown in Figure E-3 was used to determine subcarrier output level change as a function of input. This test was performed on the 57 MHz (after first conversion) subcarrier only*. Figure E-4 is a plot of the results. This is seen to be an extension of one of the curves of Figure E-2 to lower C_{in} values.

The same set-up, without the AGC-swamping signal generator, was then used to measure the subcarrier to reradiated-noise-density ratio as a function of input level. This was done by taking wave analyzer reading on the subcarrier and then tuning away about 4 kHz, into the noise band surrounding the subcarrier. The wave analyzer filter was in the 1 kHz bandwidth mode; as a check a response plot of this filter showed a noise bandwidth within one percent of 1 kHz. Results are shown in Figure E-5.

*The stronger of the two first order subcarriers.

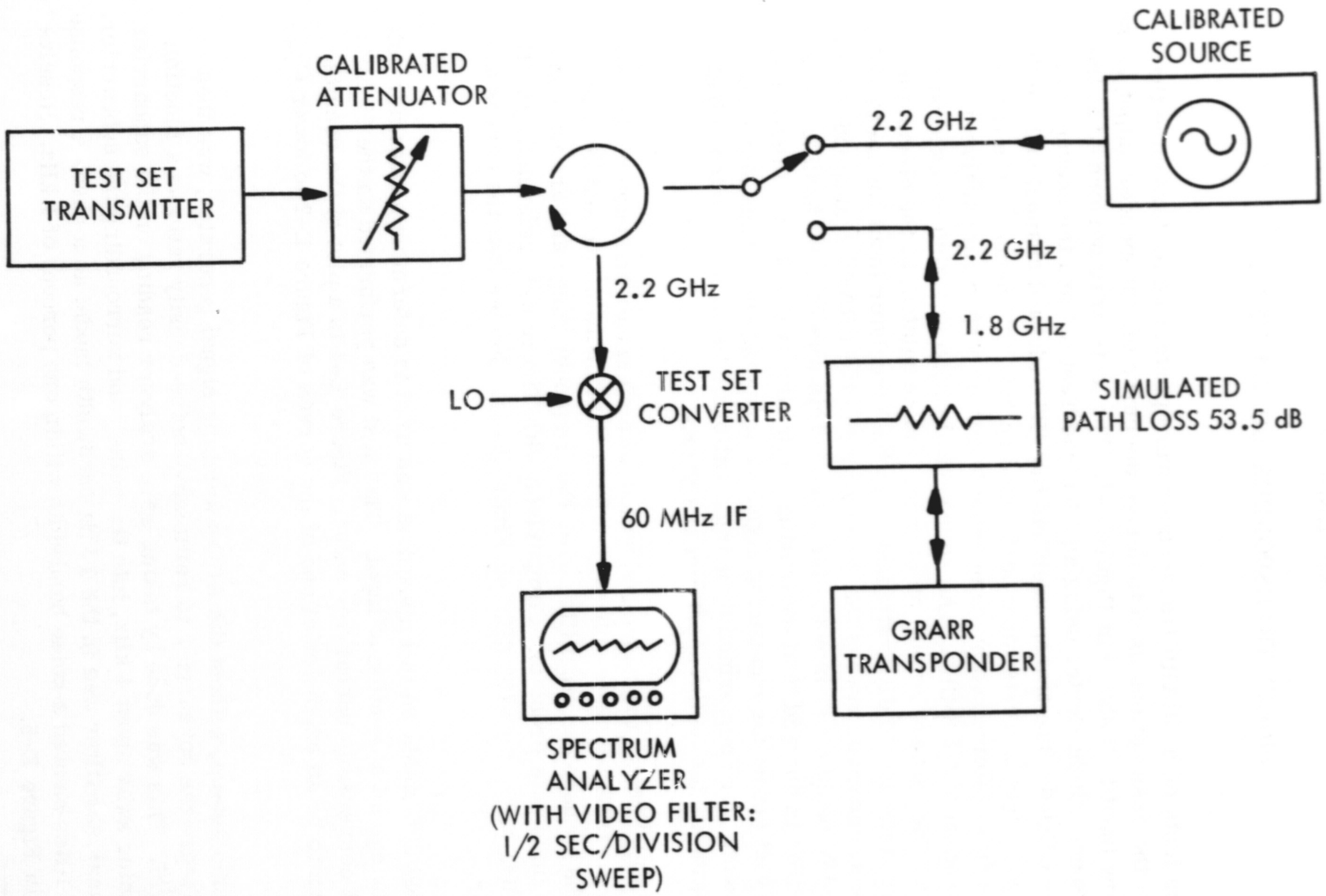

Figure E-1. Test Set-up for Measuring GRARR Transponder Signal Components Out Versus Signal In

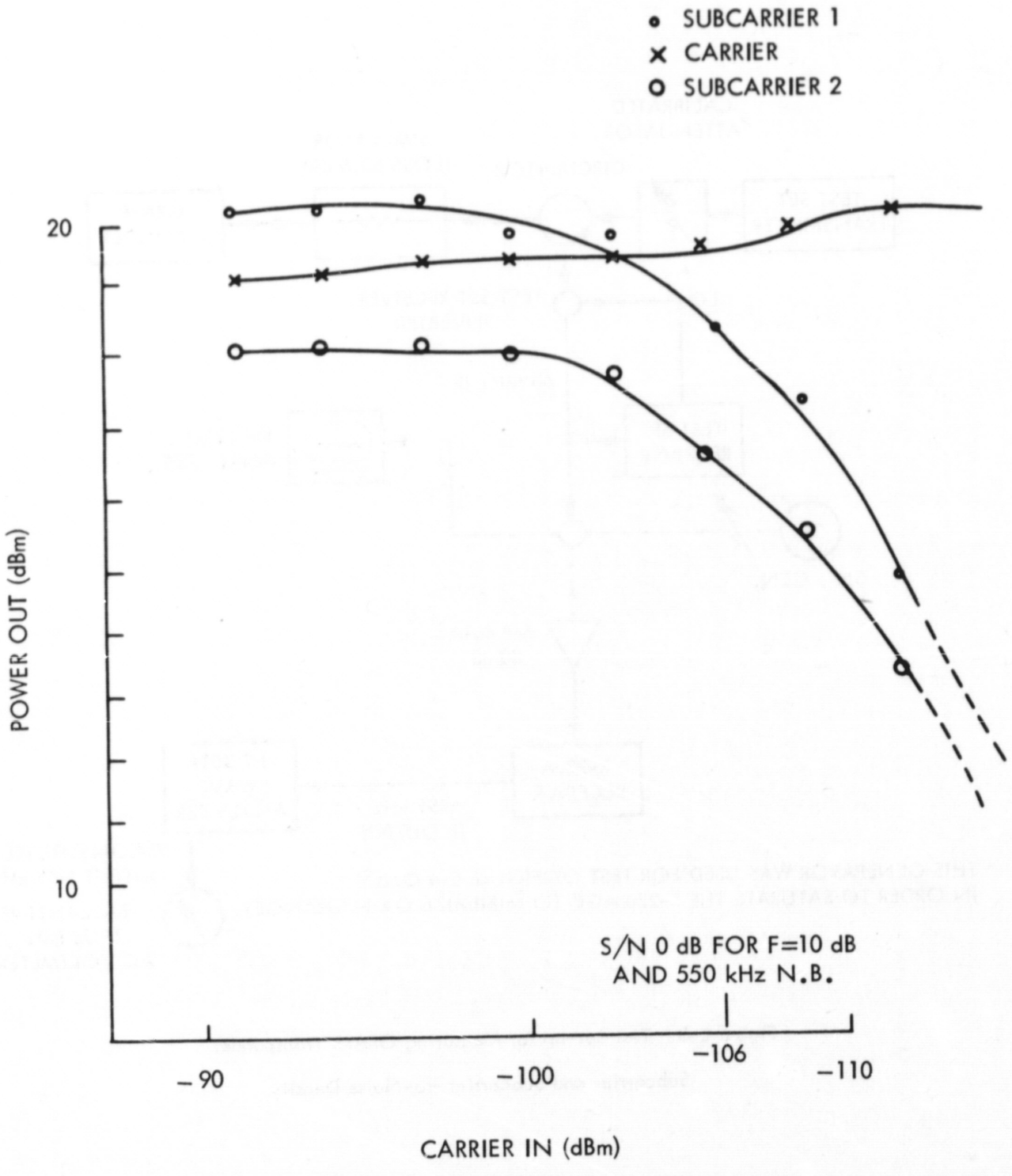

Figure E-2. GRARR Transponder Signal Components Out Versus Signal In

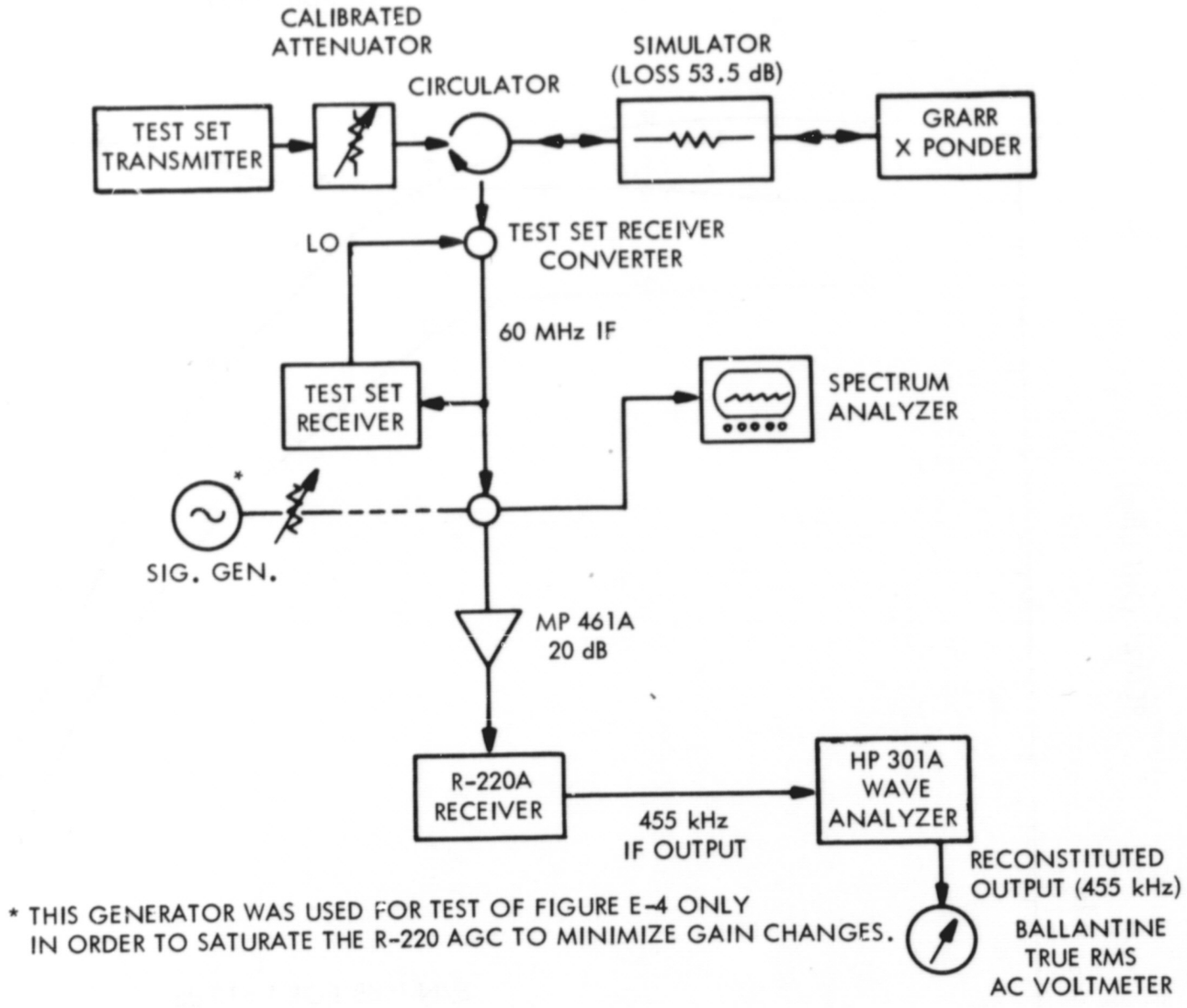

Figure E-3. Test Set-up for Measuring GRARR Transponder

Subcarrier and Subcarrier-to-Noise Density

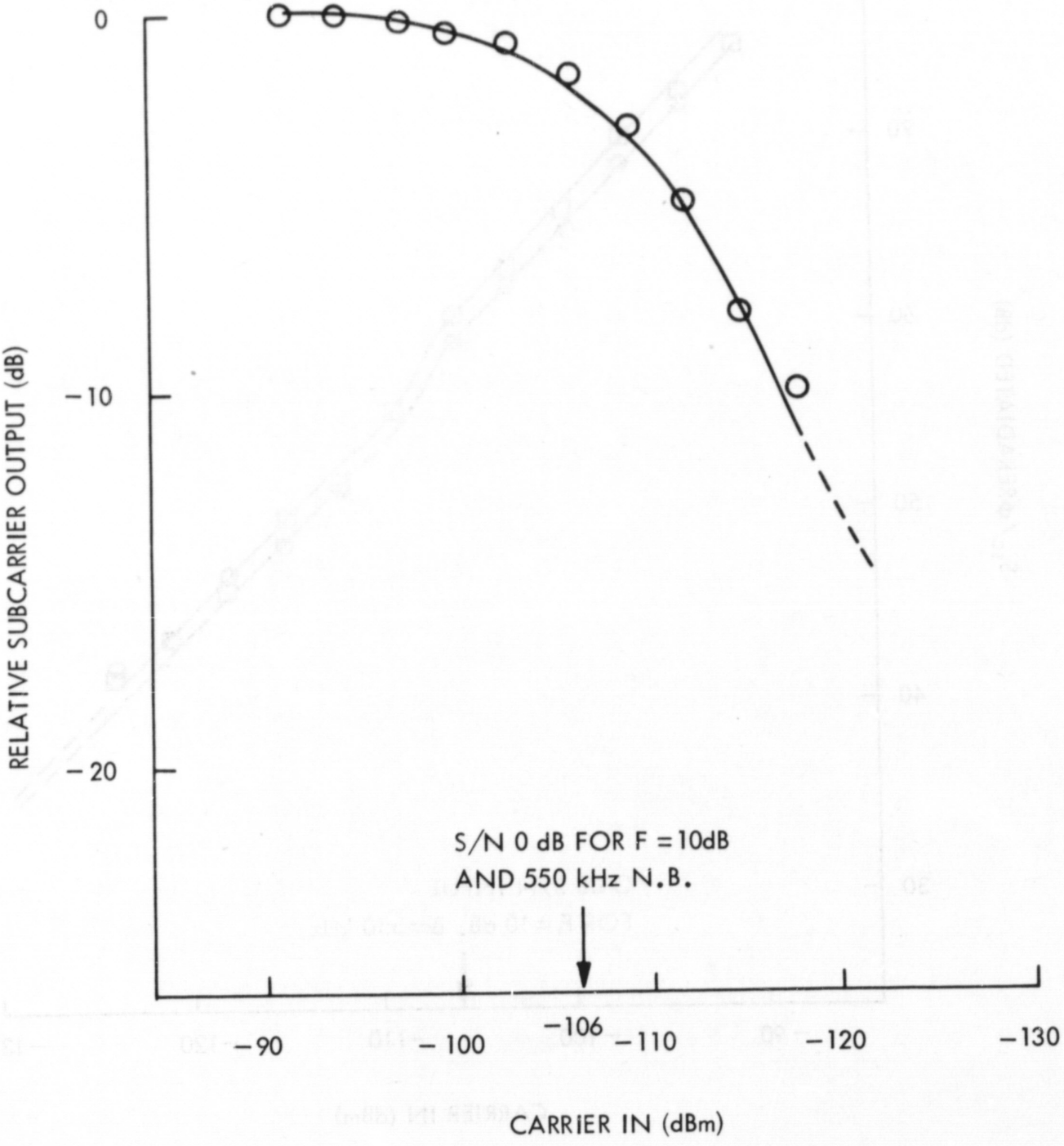

Figure E-4. GRARR Transponder Subcarrier Level Change as a Function of Input

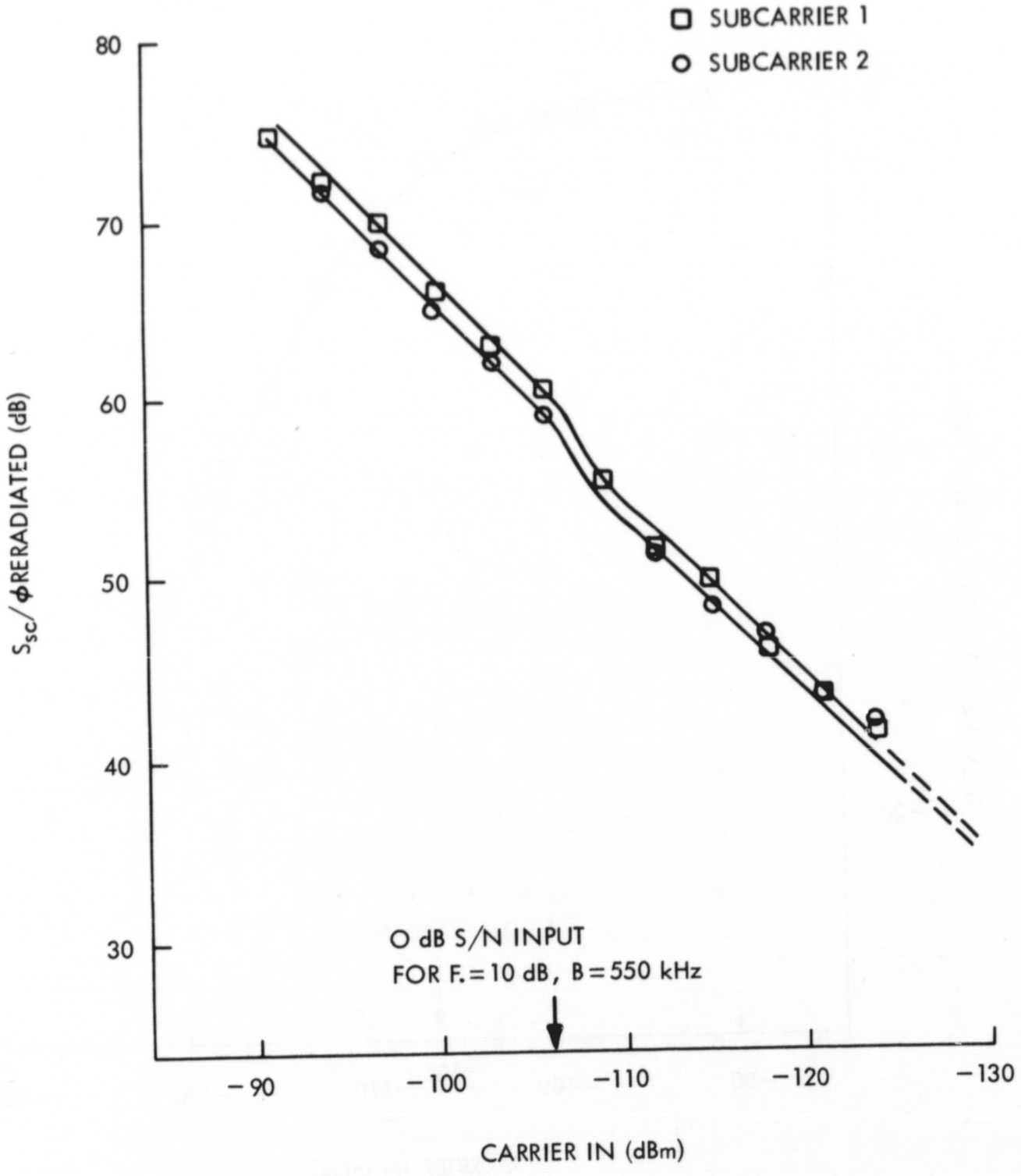

Figure E-5. GRARR Transponder Subcarrier-to-Reradiated Noise Density Ratio as a Function of Input

As a general observation, it is noted that reradiated noise behavior is as predicted by theory assuming a 10 dB transponder noise figure and a 550 kHz noise bandwidth. It should be noted that the noise spectrum around the subcarcarier is not at all flat, however, the measurements of Figure E-5 are of the noise very close to the subcarrier. The "average" noise in the 550 kHz band centered on a subcarrier is thus somewhat lower (Reference E-1).

Figure E-5 seems to indicate that the sideband signal to noise-density ratio out of the GRARR transponder is approximately the same as the transponder input signal-to-noise density ratio except at signal to noise ratios of 0 dB. Around 0 dB signal-to-noise ratio, the phase modulator and the limiter degrade the sideband signal-to-noise density ratio by 2-3 dB. Thus the data is consistent with the rationale and assumptions used in the development of the parametric power budgets.

REFERENCE

E-1 "Analysis of Signal and Noise Turnaround in the Goddard Range and Range Rate Transponder," T. J. Grenchik, GSFC X-551-69-323, August 1969.